

**EVALUATION OF TOXICITY,
PHARMACOKINETIC AND CLASTOGENICITY
PROFILE OF ETHYL 2-[4[(PIPERIDIN-1-YL)
PHENYL]-1H-BENZIMIDAZOLE-5-
CARBOXYLATE (BZD9L1), NOVEL SIRTUIN
INHIBITOR**

LEE YEUAN TING

UNIVERSITI SAINS MALAYSIA

2022

**EVALUATION OF TOXICITY,
PHARMACOKINETIC AND CLASTOGENICITY
PROFILE OF ETHYL 2-[4[(PIPERIDIN-1-YL)
PHENYL]-1H-BENZIMIDAZOLE-5-
CARBOXYLATE (BZD9L1), NOVEL SIRTUIN
INHIBITOR**

by

LEE YEUAN TING

**Thesis submitted in fulfilment of the requirements
for the degree of
Doctor of Philosophy**

May 2022

ACKNOWLEDGEMENT

I am grateful to several people for their help and guidance throughout my Ph.D. journey at the Institute for Research in Molecular Medicine (INFORMM), USM.

First of all, I would like to express my deepest gratitude to my supervisor Assoc. Prof. Dr Oon Chern Ein, for her guidance throughout these years. Thanks for her trust and for the opportunities to test new scientific hypotheses. Her support has developed me to be more independent with the ability to think outside the box. Not forget my co-supervisors: Prof. Dr Gurjeet, Assoc. Prof. Dr Sasidharan and Assoc. Prof. Dr Vikneswaran for their immense knowledge and advice in their professional field towards the completion of this study. I wish to thank Professor Yuen Kah Hay for his helpful comments during the manuscript preparation for toxicological research and his advice on pharmacokinetic experiments. My sincere thanks also go to Prof. Marco Falasca for his supervision, support, and guidance during my three-months lab attachment at CHIRI, Curtin University, Australia.

A big thank you goes to my mentor, Tan Yi Jer. I have been fortunate to have you as my mentor, teammate, and comrade over the last few years. We have gone through so many difficulties together, sharing the ups and downs, and becoming the strongest support for each other. I am also deeply indebted to the lab members, past and present: Dr. Ashwaq, Sandra, Cheng Wai Kang, Ayappa and especially Pei Yi and Deepa for their insightful opinions and assistance in my research work. Also, do not forget to the INFORMM staff and members, the students from Prof. Dr. Vikneswaran's Lab, and others who help me directly and indirectly throughout the journey. Special dedication goes to Mr Bryan Lim Chu Chwen and Ms Stasey Lynn R. Lopez for

proofreading my thesis. You have all helped, trained, and challenged me to become a better scientist. I don't know how I would have made it through all this without you.

This project is also not possible without the assistance of the late Prof. Tan Soo Choon regarding the compound synthesis and his advice on the compound formulation as well as the pharmacokinetic study. Furthermore, I would also like to thank Usains Biomics Laboratory Testing Services Sdn Bhd for providing the facilities required to synthesise BZD9L1. Special thanks to Mr. Giuseppe from Curtin University, Mr. Yeoh Seng Hoe, and Ms. Khoo Hooi Tee for their kind help with HPLC troubleshooting. My deep gratitude also goes to Dr Warren Lee for his insightful comments and provides me with immediate assistance whenever necessary. Not forgetting to express my profound thanks to my thesis committee. You have been a great source of critical feedback that has helped me strengthen my thesis and manuscript.

I must also acknowledge USM Graduate Assistantship, Malaysia Ministry of Higher Education under the Fundamental Research Grant Scheme (FRGS) grant, and Agilent Technologies Industry-Academic Collaborative Grant for financial support. This work also received financial support from Universiti Sains Malaysia Bridging Grant (304/CIPPM/ 6316520). Additionally, I would like to thank the Postgraduate Research Attachment (PGRA) for funding my three-month research attachment at the Curtin Health Innovation Research Institute (CHIRI), Curtin University, Australia.

Most importantly, I must thank my friends and family for their constant encouragement, support, and being my biggest cheerleaders throughout this journey. In addition, I am eternally grateful for everything my parents have done to support me and for your unconditional love through it all. Last but not least, I would like to thank myself for never giving up and keeping myself passionate to complete this dissertation. Thank you.

TABLE OF CONTENTS

ACKNOWLEDGEMENT.....	ii
TABLE OF CONTENTS.....	iv
LIST OF TABLES.....	xv
LIST OF FIGURES.....	xix
LIST OF SYMBOLS AND ABBREVIATION.....	xxiv
LIST OF APPENDICES.....	xxxii
ABSTRAK.....	xxxiii
ABSTRACT.....	xxxv
CHAPTER 1 INTRODUCTION AND LITERATURE REVIEW.....	1
1.1 Introduction.....	1
1.2 Literature review.....	3
1.2.1 Molecular targeted therapies.....	4
1.2.2 Sirtuins (SIRTs).....	6
1.2.3 SIRTs expression in mouse.....	20
1.2.4 Limitations of commercially available SIRT inhibitors.....	21
1.2.5 Benzimidazole as anticancer agents.....	22
1.2.6 Toxicology.....	24
1.2.6(a) Pharmaceutical toxicology.....	25
1.2.6(b) Element of toxicity.....	26
1.2.6(c) Toxicity effects.....	28
1.3 BZD9L1.....	29
1.4 Research rationale.....	32
1.5 Research objectives.....	33
1.6 Experimental design.....	34

CHAPTER 2	GENERAL TOXICOLOGY (SINGLE AND REPEATED DOSE TOXICITY) ASSESSMENT OF BZD9L1 IN BALB/C MICE.....	35
2.1	Introduction.....	35
2.2	Objectives.....	36
2.3	Materials.....	37
2.3.1	Biologicals and consumables.....	37
2.3.2	Chemicals, media, and reagents.....	37
2.3.3	Instruments.....	38
2.3.4	Software.....	39
2.3.5	Test compounds.....	39
2.3.5(a)	Vehicle control (VC).....	39
2.3.5(b)	BZD9L1.....	39
2.3.6	Experimental animals.....	40
2.4	Methodologies.....	41
2.4.1	<i>In silico</i> toxicity prediction.....	41
2.4.2	Acute toxicity study.....	41
2.4.2(a)	Sighting study.....	41
2.4.2(b)	Limit-dose study.....	43
2.4.3	Subacute toxicity study.....	45
2.4.3(a)	Clinical sign and mortality.....	46
2.4.3(b)	Body weights change, food and water consumption.....	46
2.4.3(c)	Haematological and clinical biochemistry analyses.....	46
2.4.3(d)	Gross findings and organs weight.....	47
2.4.3(e)	H&E staining and histopathology analyses.....	47
2.4.4	Statistical analyses.....	48

2.5	Results.....	50
2.5.1	<i>In silico</i> prediction of BZD9L1 toxicity.....	50
2.5.1(a)	ProTox II.....	50
2.5.1(b)	admetSAR 2.0.....	50
2.5.1(c)	Quantitative Structure–Activity Relationships (QSAR)Toolbox.....	52
2.5.1(d)	pkCSM.....	53
2.5.1(e)	Vienna LiverTox Workspace.....	53
2.5.2	BZD9L1 exhibited no acute toxicity effect in BALB/c mice.....	55
2.5.2(a)	Sighting study.....	55
2.5.2(b)	Limit dose study.....	59
2.5.3	BZD9L1 demonstrated no subacute toxicity in BALB/c mice.....	64
2.5.3(a)	Physical observation and mortality.....	64
2.5.3(b)	Body weight change, food and water consumption.....	64
2.5.3(c)	Haematological and clinical biochemistry.....	72
2.5.3(d)	Relative organ weight (R.O.W), gross necropsy and histopathology analyses.....	73
2.5.4	Summary of key findings.....	104
2.6	Discussion.....	107
2.6.1	<i>In silico</i> prediction of BZD9L1 toxicity.....	107
2.6.2	<i>In vivo</i> toxicology assessment of BZD9L1 in BALB/c mice.....	112
2.6.2(a)	Acute toxicity study.....	113
2.6.2(b)	Subacute toxicity study.....	114
2.7	Conclusions.....	124

CHAPTER 3	MOLECULAR TOXICOLOGY ASSESSMENT OF MOUSE LIVER AND KIDNEY TISSUES POST-28- DAY REPEATED BZD9L1 TREATMENT.....	125
3.1	Introduction.....	125
3.2	Objectives.....	127
3.3	Materials.....	128
3.3.1	Biologicals and consumables.....	128
3.3.2	Chemicals and reagents.....	129
3.3.3	Research kits.....	130
3.3.4	Instruments.....	130
3.3.5	Software.....	131
3.3.6	Reagents preparation.....	131
3.3.6(a)	8 M Urea lysis buffer.....	131
3.3.6(b)	1.5 M Tris-HCL stock buffer for resolving gel (pH 8.8).....	131
3.3.6(c)	1.5 M Tris-HCL stock buffer for stacking gel (pH 6.8).....	132
3.3.6(d)	10× Tris-glycine running buffer (stock solution).....	132
3.3.6(e)	1× Tris-glycine running buffer (working solution).....	132
3.3.6(f)	10× Transfer buffer (stock solution).....	132
3.3.6(g)	1× transfer buffer (working solution).....	133
3.3.6(h)	10% (w/v) APS solution.....	133
3.3.6(i)	10% (w/v) SDS.....	133
3.3.6(j)	20% (w/v) SDS.....	133
3.3.6(k)	5% skimmed milk.....	133
3.3.6(l)	Preparation of SDS-PAGE resolving gel solution.....	134

3.3.6(m)	Preparation of SDS-PAGE stacking gel solution.....	134
3.3.6(n)	1× TBS solution.....	134
3.3.6(o)	1× TBS-Tween 20 (TBST) solution.....	135
3.3.6(p)	Protein sample buffer.....	135
3.3.6(q)	Protein standard.....	135
3.3.6(r)	Ponceau S staining solution.....	135
3.3.6(s)	75% ethanol (for use in RNA extraction)	135
3.4	Methodologies.....	136
3.4.1	Protein expression study.....	136
3.4.1(a)	Protein extraction.....	136
3.4.1(b)	Protein quantification.....	137
3.4.1(c)	SDS-PAGE and Western blot.....	137
3.4.1(d)	Stripping.....	139
3.4.2	Gene expression study.....	140
3.4.2(a)	RNA extraction and quantification.....	140
3.4.2(b)	Synthesis of complementary-DNA (cDNA) from extracted RNA.....	141
3.4.2(c)	Quantitative real-time PCR (qPCR).....	141
3.4.3	Statistical analyses.....	143
3.5	Results.....	145
3.5.1	Endogenous expression of CYPs, SIRTs and organ injury markers in mice liver and kidney.....	145
3.5.1(a)	CYP proteins.....	145
3.5.1(b)	SIRT proteins.....	148
3.5.1(c)	Tissue injury markers.....	148
3.5.2	Sex-divergent expression of CYP proteins towards BZD9L1 in mouse liver but not in the kidneys.....	152

3.5.3	Differential expression of SIRT proteins in response to BZD9L1 in mouse liver and kidneys.....	158
3.5.4	Expression of tissue injury markers and cellular function markers in mouse liver and kidney tissues post BZD9L1 treatment.	165
3.6	Discussion.....	171
3.6.1	Effects of BZD9L1 on mouse liver and kidney CYPs profile.....	172
3.6.2	Effects of BZD9L1 on mouse liver and kidney SIRTs profile.	179
3.6.3	Effects of BZD9L1 on the expression of tissue injury and cellular function markers in mouse liver and kidney tissues.....	183
3.7	Conclusions.....	185
CHAPTER 4 IN VIVO ASSESSMENT OF GENOTOXICITY (CLASTOGENICITY) RISK OF BZD9L1.....		187
4.1	Introduction.....	187
4.2	Objective.....	188
4.3	Materials.....	189
4.3.1	Biologicals and consumables.....	189
4.3.2	Chemicals, media, and reagents.....	189
4.3.3	Instruments.....	190
4.3.4	Software.....	190
4.3.5	Reagents preparation.....	190
4.3.5(a)	Giemsa stain stock solution.....	190
4.3.5(b)	Giemsa stain working solution.....	190
4.3.5(c)	Diluted May-Grunwald stain solution.....	191
4.3.5(d)	0.1M phosphate buffer (pH 6.8).....	191
4.3.5(e)	Colchicine.....	191
4.3.5 (f)	0.075 M KCl.....	191

	4.3.5 (g) Carnoy's fixative solution.....	191
4.3.6	Test compounds.....	191
	4.3.6(a) Vehicle control.....	191
	4.3.6(b) BZD9L1.....	192
	4.3.6(c) Cyclophosphamide (CP).....	192
4.3.7	Experimental animals.....	192
4.4	Methodologies.....	193
	4.4.1 Bone marrow chromosomal aberration assay.....	193
	4.4.2 Bone marrow micronucleus assay.....	196
	4.4.3 Statistical analyses.....	197
4.5	Results.....	199
	4.5.1 BZD9L1 did not induce chromosomal aberration in mouse bone marrow.....	199
	4.5.2 BZD9L1 did not induce micronucleus in mouse bone marrow.	205
4.6	Discussion.....	208
	4.6.1 Chromosomal aberration evaluation.....	208
	4.6.2 Bone marrow micronucleus assessment.....	211
4.7	Conclusions.....	212
	CHAPTER 5 <i>IN VITRO</i> MITOCHONDRIAL TOXICITY ASSESSMENT IN NORMAL LIVER AND KIDNEY CELLS.....	213
5.1	Introduction.....	213
5.2	Objectives.....	215
5.3	Materials.....	216
	5.3.1 Biologicals and consumables.....	216
	5.3.2 Chemicals, media, and reagents.....	217
	5.3.3 Research kits.....	217

5.3.4	Instruments.....	217
5.3.5	Software.....	218
5.3.6	Reagents preparation.....	218
5.4	Methodologies.....	219
5.4.1	Cell culture.....	219
5.4.1(a)	Subculturing.....	219
5.4.1(b)	Cryopreservation: freezing and recovering cells.....	220
5.4.1(c)	Cell counting.....	220
5.4.1(d)	Cell treatment.....	221
5.4.2	Cell viability assays.....	221
5.4.3	Mito Stress Test assay.....	222
5.4.4	Protein expression studies.....	227
5.4.4(a)	Protein extraction and quantification.....	227
5.4.4(b)	SDS-PAGE and Western blot.....	227
5.4.5	Statistical analyses.....	228
5.5	Results.....	229
5.5.1	Effects of BZD9L1 on THLE-2 and HEK 293 cell viability and cell death.....	229
5.5.2	Effects of BZD9L1 on the bioenergetics profile of THLE-2 and HEK 293 cells.....	232
5.5.3	Effects of BZD9L1 on the regulation of mitochondrial SIRTs in THLE-2 and HEK293 cells.....	235
5.6	Discussion.....	239
5.6.1	Effects of BZD9L1 on mitochondrial functions.....	240
5.6.2	Effects of BZD9L1 on mitochondrial SIRT proteins expression.....	246
5.7	Conclusions.....	250

CHAPTER 6	DEVELOPMENT OF A SIMPLE HIGH- PERFORMANCE LIQUID CHROMATOGRAPHIC (HPLC) METHOD WITH FLUORESCENCE DETECTION FOR QUANTIFICATION OF PLASMA BZD9L1 AND ITS APPLICATION IN AN ORAL ABSORPTION STUDY OF BZD9L1 IN RAT.....	252
6.1	Introduction.....	252
6.2	Objectives.....	254
6.3	Materials.....	255
6.3.1	Biologicals and consumables.....	255
6.3.2	Chemicals and reagents.....	255
6.3.3	Instruments.....	256
6.3.4	Software.....	256
6.3.5	Compound and mobile phase preparation	257
6.3.5(a)	Preparation of the mobile phase [methanol: water (75:25)]	257
6.3.5(b)	Preparation of BZD9L1 stock and working solutions for HPLC analysis.....	257
6.3.5(c)	Preparation of calibrator for HPLC analysis.....	257
6.3.5(d)	Preparation of pure standard solution (PS) for HPLC analysis.....	257
6.3.5(e)	Preparation of quality control (QC) for HPLC analysis.....	258
6.3.5(f)	Preparation of BZD9L1 for the PK study.....	258
6.3.6	Experimental animals.....	258
6.3.7	HPLC instrumentation.....	259
6.4	Methodologies.....	260
6.4.1	BZD9L1 purity.....	260
6.4.2	Sample preparation and plasma deproteinisation.....	260
6.4.3	Development of HPLC methods for quantification of plasma BZD9L1.....	262

6.4.4	HPLC method validation for quantification of plasma BZD9L1	262
6.4.4(a)	Limits of plasma blanks/ selectivity.....	263
6.4.4(b)	Limit of detection (LoD) and limit of quantification (LoQ).....	263
6.4.4(c)	Linearity and calibration curve.....	264
6.4.4(d)	Intra-day and inter-day assay reproducibility....	264
6.4.5	<i>In vivo</i> oral absorption of BZD9L1	265
6.5	Results.....	268
6.5.1	BZD9L1 purity.....	268
6.5.2	HPLC method development for quantification of plasma BZD9L1	269
6.5.3	HPLC method validation for quantification of plasma BZD9L1	270
6.5.4	<i>In vivo</i> oral absorption of BZD9L1	275
6.6	Discussion.....	277
6.6.1	HPLC method development and validation for quantification of plasma BZD9L1.....	277
6.6.2	Oral absorption of BZD9L1.....	278
6.7	Conclusions.....	281
	CHAPTER 7 CONCLUSION AND FUTURE PERSPECTIVES.....	282
7.1	Overview.....	282
7.2	Limitations and challenges of the study.....	286
7.3	Thoughts and future direction for BZD9L1 development.....	288
7.3.1	Specificity, binding mechanism, and off-target toxicity of BZD9L1	288
7.3.2	Formulation, PK, and GLP toxicity studies.....	289
7.3.3	Exploration of other potential mechanisms of BZD9L1 in cancer.....	290
7.4	Conclusions.....	291

REFERENCES..... 295

APPENDICES

LIST OF PUBLICATIONS AND CONFERENCE PROCEEDINGS

LIST OF TABLES

		Page
Table 1.1	Chemical properties of BZD9L1.....	30
Table 2.1	List of biological and consumables.....	37
Table 2.2	List of chemicals and reagents.....	37
Table 2.3	List of instruments.....	38
Table 2.4	List of software.....	39
Table 2.5	Amount of BZD9L1 required for each treatment dose for mouse at 25 g.....	40
Table 2.6	<i>In silico</i> toxicity prediction of BZD9L1 using admetSAR 2.0...	52
Table 2.7	<i>In silico</i> toxicity prediction of BZD9L1 using QSAR Toolbox...	53
Table 2.8	Cage side behavioural abnormality observation to BALB/c mice in sighting study.	55
Table 2.9	Mean body weight and percentage of body weight change of BALB/c mice in sighting study.	56
Table 2.10	Absolute organ weight in BALB/c mice post-treatment with BZD9L1 in sighting study.	57
Table 2.11	Relative organ weight change in BALB/c mice post-treatment with BZD9L1 in sighting study.	57
Table 2.12	Clinical sign observation in BALB/c mice post single limit dose of BZD9L1 treatment.	60
Table 2.13	Mean body weight change of BALB/c mice post single limit dose of BZD9L1 treatment.	60
Table 2.14	Absolute and relative organ weight of BALB/c mice post single limit dose of BZD9L1 treatment.	61
Table 2.15	Clinical sign and behavioural observation to BALB/c mice following repeated dose of BZD9L1 treatment.....	65
Table 2.16	Mean body weight change of BALB/c mice following repeated dose oral administration of BZD9L1.....	66
Table 2.17	Percentage of body weight change of BALB/c mice following repeated dose oral administration of BZD9L1.....	67

Table 2.18	Food consumption of BALB/c mice during the repeated dose toxicity study.	69
Table 2.19	Water intake of mice during the repeated dose toxicity study....	70
Table 2.20	Haematological parameters of male mice following 28 days repeated dose oral administration of BZD9L1	75
Table 2.21	Haematological parameters of female mice following 28 days repeated dose oral administration of BZD9L1	76
Table 2.22	Haematological parameters of total mice following 28 days repeated dose oral administration of BZD9L1	77
Table 2.23	Serum biochemistry in male mice following 28 days repeated dose oral administration of BZD9L1	80
Table 2.24	Serum biochemistry in female mice following 28 days repeated dose oral administration of BZD9L1	81
Table 2.25	Serum biochemistry in total mice following 28 days repeated dose oral administration of BZD9L1	82
Table 2.26	Absolute organ weight in BALB/c mice following 28 days repeated dose oral administration of BZD9L1	87
Table 2.27	Relative organ weight change in BALB/c mice following 28 days repeated dose oral administration of BZD9L1	89
Table 2.28	Summary of <i>in silico</i> prediction of BZD9L1 toxicity using ProTox II, AdmetSAR 2.0, QSAR Toolbox, pkCSM and Vienna LiverTox.	104
Table 3.1	List of biological and consumables.....	128
Table 3.2	List of chemicals, media, and reagents.....	129
Table 3.3	List of research kits and arrays.....	130
Table 3.4	List of instruments.....	130
Table 3.5	List of software.	131
Table 3.6	The preparation of resolving gel with different percentage (2 gels).....	134
Table 3.7	The preparation of stacking gel (2 gels)	134
Table 3.8	List of primary antibodies.....	138
Table 3.9	List of primer sequences.	142

Table 3.10	Summary of CYPs protein expression between females, males and total in the liver and kidneys post 28-day repeated oral dose of BZD9L1 treatment.	157
Table 3.11	Summary SIRT protein expression between females, males and total in the liver and kidneys post 28-day repeated oral dose of BZD9L1 treatment.	164
Table 4.1	List of biological and consumables.....	189
Table 4.2	List of chemicals, media, and reagents.....	189
Table 4.3	List of instruments.	190
Table 4.4	List of software.	190
Table 4.5	Total chromosomal aberration and mitotic index of female bone marrow cells treated with BZD9L1.....	201
Table 4.6	Total chromosomal aberration and mitotic index of male bone marrow cells treated with BZD9L1 at limit dose.....	203
Table 4.7	Effects of BZD9L1 on the PCE/(PCE + NCE) ratio and micronuclei in mouse bone marrow.	206
Table 5.1	List of biological and consumables.....	216
Table 5.2	List of chemicals, media, and reagents.....	217
Table 5.3	List of research kits.....	217
Table 5.4	List of instruments.	218
Table 5.5	List of software.	218
Table 5.6	Seahorse XF DMEM assay medium composition.....	222
Table 5.7	Stock solutions of oligomycin, FCCP, and rotenone/antimycin A.....	223
Table 5.8	Working solution of oligomycin, FCCP and rotenone/antimycin A.....	223
Table 5.9	List of the equation derived from Mito Stress Test profile for mitochondrial functions measurement.....	226
Table 5.10	List of primary antibodies.	227
Table 5.11	IC ₅₀ of BZD9L1 in THLE-2 and HEK 293 cells at 24, 48 and 72 h of treatment.	229
Table 6.1	List of biological and consumables.....	255

Table 6.2	List of chemicals and reagents.....	255
Table 6.3	List of instruments.	256
Table 6.4	List of software.	256
Table 6.5	The HPLC instrument parameters and conditions used in the method validation and analyses.....	259
Table 6.6	Parameters investigated in the development of the HPLC method for the analysis of BZD9L1 in plasma.....	262
Table 6.7	Calibration results of BZD9L1 analysed by HPLC-fluorescence detection.	272
Table 6.8	Recovery, intra-day, and inter-day accuracy and precision values for BDZ9L1 spiked in rat plasma.....	274
Table 6.9	Summary of PK parameters following a single oral dose of BZD9L1 at 250 mg/kg in the rat.	275
Table 7.1	Summary of key findings and the impacts.....	293
Table A1	List of animal ethics approval for each animal study.....	341
Table B1	Haematological and clinical chemistry parameters in untreated mice.	350

LIST OF FIGURES

	Page
Figure 1.1 Overview of the molecular targeted therapy mechanism.....	6
Figure 1.2 Representative SIRT structure.....	7
Figure 1.3 Enzymatic activities of SIRT deacetylation.....	10
Figure 1.4 SIRT4 and SIRT6 exhibit ADP-ribosyl transferase activity.....	11
Figure 1.5 Enzymatic activities of SIRT deacylation.....	12
Figure 1.6 The 23 isoforms of SIRTs (SIRT1-7)	13
Figure 1.7 Overview of localisation, class and enzyme activities, and various isoforms of SIRT1-7.	14
Figure 1.8 Structure and tautomerism of benzimidazole.....	23
Figure 1.9 Steps of non-clinical studies in the drug development process.	26
Figure 1.10 Overview of the flow by which toxicity occurs.....	29
Figure 1.11 Structure of BZD9L1.....	30
Figure 1.12 Overview of the experimental design	34
Figure 2.1 Illustration of acute sighting and limit-dose studies experimental flow.	44
Figure 2.2 Illustration of subacute toxicity study experimental flow.....	49
Figure 2.3 <i>In silico</i> toxicity prediction of BZD9L1 using ProTox II software.	51
Figure 2.4 <i>In silico</i> toxicity prediction of BZD9L1 using pkCSM software.	54
Figure 2.5 <i>In silico</i> drug-induced liver injury (DILI) prediction using Vienna LiverTox.	54
Figure 2.6 (A) Mean body weight and (B) percentage of body weight change of female BALB/c mice in sighting study.....	56
Figure 2.7 Absolute and relative organ weight in BALB/c mice post-treatment with BZD9L1 in sighting study.....	57
Figure 2.8 Histopathological examination of key organs post treatment with BZD9L1 in sighting study.	58

Figure 2.9	Mean and relative body weight change of female mice post single limit dose of BZD9L1.	61
Figure 2.10	Absolute and relative organ weight of mice post single limit dose of BZD9L1.	62
Figure 2.11	Histopathological examination of key organs post single limit dose of BZD9L1.	63
Figure 2.12	Effects of subacute oral administration of BZD9L1 on mean body weight and percentage of body weight change in BALB/c mice.	68
Figure 2.13	Food consumption and water intake of BALB/c mice in the 28 days repeated oral dose toxicity study.....	71
Figure 2.14	Effects of subacute oral administration of BZD9L1 on haematology parameters in BALB/c mice.....	78
Figure 2.15	Effects of subacute oral administration of BZD9L1 on haematology parameters (white blood cells profile and platelets) in BALB/c mice.....	79
Figure 2.16	Effects of subacute oral administration of BZD9L1 on electrolyte and renal profile in BALB/c mice.....	83
Figure 2.17	Effects of subacute oral administration of BZD9L1 on serum proteins in BALB/c mice.	84
Figure 2.18	Effects of subacute oral administration of BZD9L1 on serum lipid profile in BALB/c mice.	85
Figure 2.19	Effects of subacute oral administration of BZD9L1 on liver enzyme in BALB/c mice.	86
Figure 2.20	Absolute organ weight change in BALB/c mice following 28 days repeated dose oral administration of BZD9L1.....	88
Figure 2.21	Relative organ weight of BALB/c mice following 28 days repeated dose oral administration of BZD9L1.....	90
Figure 2.22	Gross necropsy of key organs in mice following 28 days repeated dose oral administration of BZD9L1.....	91
Figure 2.23	Macroscopic observation of key organs in the male mice following 28 days repeated dose oral administration of BZD9L1.	93
Figure 2.24	Macroscopic observation of key organs in the female mice following 28 days repeated dose oral administration of BZD9L1.	94

Figure 2.25	Histopathology examination of the heart of female and male mice following 28 days repeated dose oral administration of BZD9L1.	95
Figure 2.26	Histopathology examination of the lungs of female and male mice following 28 days repeated dose oral administration of BZD9L1.	96
Figure 2.27	Histopathology examination of the kidneys of female mice following 28 days repeated dose oral administration of BZD9L1.	98
Figure 2.28	Histopathology examination of stomach of female mice following 28 days repeated dose oral administration of BZD9L1.	99
Figure 2.29	Histopathology examination of the intestine of female mice following 28 days repeated dose oral administration of BZD9L1.....	100
Figure 2.30	Histopathology examination of spleen of female mice following 28 days repeated dose oral administration of BZD9L1.	101
Figure 2.31	Histopathology examination of liver of female mice following 28 days repeated dose oral administration of BZD9L1.....	102
Figure 2.32	Histopathology examination of the organ of male mice following repeated dose with intraperitoneal injection of 50 mg/kg BZD9L1.	103
Figure 3.1	Illustration of protein analysis on mice liver and kidney tissues experimental flow.	139
Figure 3.2	Illustration of gene analysis on mice liver and kidney tissues experimental flow.	144
Figure 3.3	Endogenous expression of mouse hepatic and renal Cytochrome P450 (CYP) proteins	146
Figure 3.4	Endogenous expression of mouse hepatic and renal SIRT1-7 protein.....	149
Figure 3.5	Endogenous expression of liver and kidney injured markers in mice.....	151
Figure 3.6	Cytochrome P450 (CYP) protein expression profile in mouse liver tissues post BZD9L1 treatment.....	153
Figure 3.7	Cytochrome P450 (CYP) protein expression profile in mouse kidney tissues post BZD9L1 treatment.	155

Figure 3.8	BZD9L1-regulated SIRT1-7 protein expression in mouse liver tissues.....	160
Figure 3.9	BZD9L1-regulated SIRT1-7 protein expression in mouse kidney tissues.....	162
Figure 3.10	BZD9L1-regulated organ injury markers in mouse liver tissues.	166
Figure 3.11	BZD9L1-regulated organ injury markers in mouse kidney tissues.....	167
Figure 3.12	Gene expression profile of toxicity markers in mouse liver tissues post BZD9L1 treatment.....	169
Figure 3.13	Gene expression profile of toxicity markers in mouse kidney tissues post BZD9L1 treatment.....	170
Figure 4.1	Illustration of the experimental flow of the <i>in vivo</i> bone marrow chromosomal aberration assay.....	195
Figure 4.2	Illustration of the experimental flow of the <i>in vivo</i> bone marrow micronucleus assay.	198
Figure 4.3	Representative images of chromosomal structural aberrations detected in mice after treatment.	200
Figure 4.4	Effects of BZD9L1 in female bone marrow chromosomal structural aberrations and mitotic index.	202
Figure 4.5	Effects of BZD9L1 in male bone marrow chromosomal structural aberrations and mitotic index.	204
Figure 4.6	Effects of BZD9L1 on frequency of PCE and micronucleus in <i>in vivo</i> bone marrow micronucleus assay.	207
Figure 5.1	Illustration of Mito Stress Test assay experiment flow.....	225
Figure 5.2	Bioenergetic profile of Cell Mito Stress Test using the Agilent Seahorse XF platform, showing the critical parameters for mitochondria function.	226
Figure 5.3	Effects of BZD9L1 on normal liver and kidney cell viability....	229
Figure 5.4	The expression of apoptotic marker cleaved-PARP in THLE-2 and HEK 293 cells post-BZD9L1 treatment.....	231
Figure 5.5	The effects of BZD9L1 on oxygen consumption (OCR) and extracellular acidification rate (ECAR) measurement in THLE-2 cells.	233

Figure 5.6	The effects of BZD9L1 on oxygen consumption rate (OCR) and extracellular acidification rate (ECAR) measurement in HEK293 cells.	234
Figure 5.7	SIRT proteins expression change in normal human liver cells post-BZD9L1 treatment.	236
Figure 5.8	SIRT proteins expression change in normal human kidney cells post-BZD9L1 treatment.	238
Figure 5.9	Illustration of the changes in the mitochondrial OXPHOS upon injection of Mito Stress Test kit.....	242
Figure 5.10	Overview of mitochondrial SIRT3-5 in regulating various mitochondrial functions.....	246
Figure 6.1	Illustration of the working solution and sample preparation flow	261
Figure 6.2	Schematic diagram of oral absorption study design	267
Figure 6.3	Peak purity of BZD9L1 determined by HPLC-DAD method....	268
Figure 6.4	Chromatogram of pure standard and plasma spiked with BZD9L1.	271
Figure 6.5	Standard calibration curve of plasma spiked with BZD9L1.....	272
Figure 6.6	Chromatograms from the analysis of BZD9L1.....	273
Figure 6.7	Mean plasma BZD9L1 concentration-time curve.....	276
Figure C1	Histopathology examination of the organs of untreated mice...	351
Figure C2	Histopathology examination of the organ of male mice after 28 days of repeated oral administration of 1000 mg/kg BZD9L1...	352
Figure D1	HPLC chromatograms of BZD9L1 were detected by fluorescence (λ_{Ex} : 346 nm, λ_{Em} : 448 nm) and UV (342 nm) detectors.	353
Figure D2	Preliminary screening of HPLC mobile phases.....	354
Figure D3	HPLC chromatograms of BZD9L1 run with different mobile phases.	355
Figure D4	Detection limit of BZD9L1.	356
Figure D5	Solvent optimisation for plasma BZD9L1 deproteinisation.....	357

LIST OF SYMBOLS AND ABBREVIATIONS

%	Percentage
&	Ampersand (represent and)
<	Less than
>	Greater than
±	Plus-minus sign
×g	Times gravity
≤	Less than or equal to
≥	Greater than or equal to
µg*h/mL	Unit for area under the curve
µg/mL	micrograms/milliliter
µM	Micromolar
5-FU	5-fluorouracil
∞	Infinity
Å	Angstrom
ABC	ATP-binding cassette protein
A Log P	Partition Coefficient
A.O.W	Absolute organ weight
ADME	Absorption, distribution, metabolism, excretion
ADR	Adverse drug reaction
ALB/GLB	Albumin/ Globulin
ALP	Alkaline phosphatase
ALT	Alanine aminotransferase
ANOVA	Analysis of variance
ANT	Adenine nucleotide translocase
AP	Active pharmaceutical
AR	Analytical Reagent
ARASC	Animal Research and Service Centre,
AST	Aspartate transaminase
ATP	Adenosine triphosphate
AUC	Area under the plasma concentration curve
AUC _{0-∞}	Area under the plasma concentration-time curve· from time zero to infinity

AUC _{0-t}	Area under the plasma concentration curve from time zero to last sampling time, t
B	Break (International System for Human Cytogenetic nomenclature)
b.w.	Body weight
BALB/c	Bagg Albino coat with genotype c
BCA	Bicinchoninic acid
BEGM	Bronchial Epithelial Cell Growth Medium
BSA	Bovine serum albumin
BSEP	Bile Salt Export Pump
BWL	Body weight loss
°C	Degree Celsius
C.I.	Confidence interval
C.V.	Coefficient of variation
CBB	Coomassie Brilliant Blue
cDNA	Complementary deoxyribonucleic acid
chol	Cholesterol
CF	Centric fusion (International System for Human Cytogenetic nomenclature)
CLU	Clusterin- α
C _{max}	Peak plasma concentration
CMC	Sodium carboxymethyl cellulose
CO ₂	Carbon dioxide
CP	Cyclophosphamide
CRC	Colorectal cancer
Csb	Chromosome break (International System for Human Cytogenetic nomenclature)
CT	Cycle threshold
Ctb	Chromatid break
CYP	Cytochrome P450 subfamily
CYP1A1	Cytochrome P450 subfamily 1a1 (Orthologous to human CYP1A1)
CYP1A2	Cytochrome P450 subfamily 1a2 (Orthologous to human CYP1A2)
CYP26A1	Cytochrome P450 subfamily 26a1 (Orthologous to human CYP26A1)
CYP2A5	Cytochrome P450 subfamily 2a5 (Orthologous to human CYP2A6)
CYP2D	Cytochrome P450 subfamily 2d (Orthologous to human CYP2D6)
CYP2E1	Cytochrome P450 subfamily 2e1 (Orthologous to human CYP2E1)

CYP3A11	Cytochrome P450 subfamily 3a11 (Orthologous to human CYP3A4)
CYP4A10/A12/A14	Cytochrome P450 subfamily 4a10/a12/a14 (Orthologous to human CYP4A1/A2/A3)
D/T	Death/ Treated
Da	Dalton
DAD	Diode Array Detector
ddH ₂ O	Double distilled water
del	Deletion (International System for Human Cytogenetic nomenclature)
dH ₂ O	Distilled water
Dic	Dicentric
DILI	Drug-induced liver injury
DMEM	Dulbecco's Modified Eagle Medium
DMSO	Dimethyl sulfoxide
DNA	Deoxyribonucleic acid,
DPX	Dibutylphthalate Polystyrene Xylene
e.g.	exempli gratia (for example)
ECAR	Extracellular acidification rate
EE	End-to-end association
EMH	Extramedullary hematopoiesis
EPA	United States Environmental Protection Agency
ERK	Extracellular-signal-regulated kinase
ETC	Electron transport chain
F	Fragment (International System for Human Cytogenetic nomenclature)
F %	Oral bioavailability
FADH ₂	flavin adenine dinucleotide
FBS	Foetal bovine serum
FCCP	Carbonyl cyanide-p-trifluoromethoxyphenylhydrazone
FDA	U.S. Food and Drug Administration
G	Gap (International System for Human Cytogenetic nomenclature)
g	Gram
g/mol	Unit of molar mass
GAPDH	Glyceraldehyde-3-phosphate dehydrogenase
GC	Gas chromatography

GH	Growth hormone
GHS	Globally Harmonised Classification System for Chemical Substances and Mixtures.
GI	Gastrointestinal tract
GLP	Good Laboratory Practice
GOI	Genes of interest
h	Hour(s)
H&E	Hematoxylin and eosin stain
H ⁺	Proton
HD	High-dose
HEK293	Human embryonic kidney 293
Herg	Human ether-à-go-go-related gene channel
HMQC	Heteronuclear Multiple Quantum Coherence
HO-1	Heme oxygenase-1
HPLC	High performance liquid chromatography
i.e.	id est (that is)
IACUC	Institutional animal care and use committee
IC ₅₀	Half-maximal inhibitory concentration
IP	Intraperitoneal injection
ISCN	International System for Human Cytogenomic Nomenclature
IST	<i>In silico</i> toxicology
K ₂ HPO ₄	Potassium phosphate dibasic
kDa	Kilodaltons
kg	Kilogram
KH ₂ PO ₄ •H ₂ O	Anhydrous potassium phosphate monobasic
KIM-1	Kidney injury molecule 1
LCN2	Lipocalin-2
LD	Low-dose
LD ₅₀	Half-median lethal dose
LOAEL	Lowest Observed Adverse Effect
LoD	Limit of Detection
LoQ	Limit of Quantification
LU	Luminescence (or light) units
M	Molarity
MATE1	Multidrug and toxin extrusion protein 1

mAU	Milli-absorbance unit, or 0.001 absorbance units (AU)
MCH	Mean cell haemoglobin
MCHC	Mean cell haemoglobin concentration
MCV	Mean cell volume
MD	Medium-dose
MeOH	Methanol
mg	Miligram
mg/kg	Milligram of drug per kilogram of body weight.
min	Minute(s)
mL	Micro litre
mM	Micro molar
mmol/L	millimoles per litre
MNA	Micronucleus assay
MNPCE	Micronucleated polychromatic erythrocytes
mnSOD2	Manganese superoxide dismutase
MPR3	Multidrug resistance-associated protein 3
MPR4	Multidrug resistance-associated protein 4
mRNA	Messenger ribonucleic acid
MTD	Maximum tolerated dose
MTS	Mitochondrial targeting sequence
MΩ-cm	Megohm-centimeter
n or N	Number
NADH	Nicotinamide adenine dinucleotide
NAM	Nicotinamide
NAMPT	Nicotinamide phosphoribosyltransferase
NMNAT	Nicotinamide mononucleotide adenylyl transferase
NCE	New chemical entities
NCE	Normochromatic erythrocytes
NH ₃	Ammonia
NLS	Nuclear localisation signal
nm	Nanometers
NOAEL	No-Observed-Adverse-Effect level
Nqo1	NAD(P)H quinone dehydrogenase1
O.D.	Optical density

O ₂	Oxygen
OATP1B1	Organic anion transporter family member 1B1
OATP1B2	Organic anion transporter family member 1B2
OATP1B3	Organic anion transporter family member 1B3
OATPs	Organic anion transporters
OCR	Oxygen consumption rate
OCT	Organic cation transporter
OECD	Organisation for Economic Co-operation and Development
Oligo	Oligomycin A
OXPPOS	Oxidative phosphorylation
P	Pulverization
p53	Tumour protein p53
PARP	Poly (ADP-ribose) polymerase
PCE	Polychromatic erythrocytes
PCS	Premature chromatid separation
pg	Pico gram
P-gp	P-glycoprotein
pH	Potential of hydrogen
PK	Pharmacokinetic
pKa	Negative log base ten of the Ka value (acid dissociation constant)
Pol I	RNA polymerase I
PPAR γ	Peroxisome proliferator-activated receptor gamma
PS	Pure standard
PVDF	Polyvinylidene fluoride
QC	Quality control
qPCR	Quantitative polymerase chain reaction
QSAR	Quantitative structure activity relationship
R	Ring
R.O.W	Relative organ weight
r.t.	Room temperature
R ²	Mean goodness-of-fit
RBC	Red blood corpuscles
RCR	Respiratory control ratio
RDW	Red cell distribution width

RNA	Ribonucleic acid
ROS	Reactive oxygen species
Rot/AA	Rotenone, and Antimycin A
rpm	Revolutions Per Minute
S.E.M	Standard error of mean
SA	Synthetic accessibility
SAR	Structure-activity
SD	Standard deviation
SDS-PAGE	Sodium dodecyl sulfate polyacrylamide gel electrophoresis
sec	Second(s)
SEM	Standard Error of the Mean
SIRT1	Sirtuin 1
SIRT2	Sirtuin 2
SIRT3	Sirtuin 3
SIRT4	Sirtuin 4
SIRT5	Sirtuin 5
SIRT6	Sirtuin 6
SIRT7	Sirtuin7
SIRTs	Sirtuins
SMILES	Simplified Molecular Input Line Entry System
SNR	Signal-to-noise ratio
SOD1	Superoxide dismutases 1
SOD2	Superoxide dismutases 2
$t_{1/2}$	Elimination half-life
TBST	Tris-buffered saline (TBS) and Tween 20
TCA	Tricarboxylic acid
THLE-2	Transformed Human Liver Epithelial-2
TIM-1	T-cell immunoglobulin and mucin domain 1
T_{max}	Time to reach peak plasma concentration
TNF- α	Tumour necrosis factor alpha
TPSA	Topological polar surface area
U/L	Units/Litre
UCP	Uncoupling protein
ULN	Upper limit of normal

UV	Ultraviolet
V	Voltage
VC	Vehicle control
Vol	Volume
w/v	Weight over volume
WBC	White blood cells
WHO	World Health Organisation
α	Alpha
β	Beta
β -actin	Beta actin
γ	Gamma
δ	Delta
Δ	Delta
$\Delta\Delta CT$	$\text{Mean}(\Delta ct_{\text{treated}}) - \text{Mean}(\Delta ct_{\text{control}})$
λ_{Em}	Emission wavelength
λ_{Ex}	Excitation wavelength
μg	Micro gram
μm	Micro meter

LIST OF APPENDICES

- APPENDIX A ANIMAL ETHICS APPROVAL AND CERTIFICATES OF LABORATORY ANIMAL TRAINING PROGRAMMES FOR MICE AND RAT
- APPENDIX B HAEMATOLOGICAL AND CLINICAL CHEMISTRY PARAMETERS IN UNTREATED MICE.
- APPENDIX C HISTOPATHOLOGY EXAMINATION OF THE ORGANS OF UNTREATED MICE AND MALE MICE (1000 MG/KG).
- APPENDIX D HPLC METHOD DEVELOPMENT FOR PLASMA BZD9L1 SEPARATION
- APPENDIX E GLOSSARY

**PENILAIAN PROFIL KETOKSIKAN, FARMAKOKINETIK DAN
KLASTOGENIK ETHYL 2-[4(PIPERIDIN-1-YL) PHENYL]-1H-
BENZIMIDAZOLE-5-CARBOXYLATE (BZD9L1), PERENCAT SIRTUIN**

BAHARU

ABSTRAK

Sirtuins Mamalia (SIRT) dikaitkan dengan pelbagai jenis penyakit, termasuk barah, diabetes, penyakit neurodegeneratif, dan penyakit kardiovaskular. Oleh itu, SIRT adalah sasaran terapeutik yang menarik untuk pembangunan farmaseutikal. Kekurangan perencat SIRT yang berpotensi dalam ujian klinikal barah menekankan keperluan untuk mengembangkan modulator SIRT yang berkesan sebagai terapi antikanser. Penyelidikan makmal menyoroti kemampuan jenis SIRT inhibitor utama (BZD9L1) untuk merencat pertumbuhan tumor kolorektal secara *in vitro* dan *in vivo* dengan memodulasi laluan barah kanser kolorektal yang berbeza dengan profil mutasi. Tambahan pula, kesan sinergistik BZD9L1 pada *in vitro* assays dan kajian xenograf tumor apabila digabungkan dengan 5-fluorouracil (5-FU) seterusnya menyokong kesan terapeutik yang menjanjikan BZD9L1 sebagai rejimen antikanser. Walau bagaimanapun, ciri toksikologi sebatian ini masih belum diketahui. Sepengetahuan kami, proses pengaturan SIRT dalam hati dan buah pinggang oleh perencat molekul kecil dalam kajian ketoksikan ubat belum dilaporkan. Oleh itu, projek ini bertujuan untuk menentukan toksikologi, regulasi molekul terhadap ketoksikan, farmakokinetik dan profil klastogenik BZD9L1 dalam model *in vitro* atau *in vivo*. Kajian ini merangkumi penilaian ketoksikan oral akut dan subakut, penilaian ketoksikan molekul, penyimpangan kromosom sumsum tulang dan ujian mikronukleus, serta farmakokinetik oral dan penilaian ketoksikan mitokondria. Dalam kajian ketoksikan akut, BZD9L1

tidak menunjukkan tanda-tanda ketoksikan pada dos had (2000 mg/kg). Data ketoksikan subakut menyoroti Tahap Reaksi Adverse Tidak Diperhatikan (NOAEL) BZD9L1 pada dos maksimum 1000 mg/kg. Walaupun perubahan dalam parameter biokimia hematologi dan serum tertentu dalam kajian ini mungkin tidak memaparkan kepentingan biologi dan klinikal. BZD9L1 mengatur ekspresi protein SIRT1-7 dalam tisu hati dan ginjal, dan menunjukkan kesekatlakuan protein sitokrom hati P450 (CYP) 2A5 dan CYP2D secara khusus mengikut jantina. Walau bagaimanapun, BZD9L1 pada semua dos tidak mendorong ekspresi molekul penanda kerosakan organ atau mengubah penanda fungsi sel di hati dan buah pinggang selepas rawatan. BZD9L1 juga tidak menyebabkan penyimpangan kromosom dan ketoksikan sumsum tulang pada dos sehingga 1000 dan 2000 mg/kg. Lebih-lebih lagi, tidak ada perubahan pada sel darah merah polikromatik (PCE) / jumlah sel darah merah atau PCE mikronukleus diperhatikan ($p > 0.05$), dengan demikian menggambarkan BZD9L1 sebagai tidak klastogenik. Plasma yang diperoleh dari tikus Sprague Dawley pasca-rawatan dengan dos oral tunggal pada 250 mg/kg BZD9L1 menunjukkan T_{max} (waktu puncak) pada 4 jam dengan C_{max} (kadar puncak) pada 0.5 $\mu\text{g/mL}$. Secara keseluruhan, kajian ini membuktikan keselamatan BZD9L1 dalam kajian ketoksikan jangka pendek dan menekankan keperluan strategi yang diperibadikan sekiranya BZD9L1 diteruskan dalam sasaran perkembangan ubat.

**EVALUATION OF TOXICITY, PHARMACOKINETIC AND
CLASTOGENICITY PROFILE OF ETHYL 2-[4[(PIPERIDIN-1-YL)
PHENYL]-1H-BENZIMIDAZOLE-5-CARBOXYLATE (BZD9L1), NOVEL
SIRTUIN INHIBITOR**

ABSTRACT

The mammalian sirtuins (SIRT_s) have been linked to various diseases including cancer, diabetes, neurodegenerative and cardiovascular diseases. Thus, SIRT_s are attractive targets for the development of pharmaceuticals. The lack of potential SIRT inhibitors in cancer clinical trials highlights the need to develop a potent SIRT modulator as an anti-cancer therapeutic. Studies in the lab have highlighted the capability of a lead sirtuin inhibitor (BZD9L1) to reduce colorectal tumour growth *in vitro* and *in vivo* by modulating different cancer pathways in colorectal cancer with different mutation profiles. Also, synergistic effects of BZD9L1 in *in vitro* assays and tumour xenograft study when used in adjunct with 5-Fluorouracil (5-FU) further support the promising therapeutic effects of BZD9L1 as anticancer regime. Nevertheless, the toxicology profile of this compound remains unknown. To our knowledge, no prior work has reported the regulation of SIRT_s in the liver and kidney by a small molecule inhibitor in a drug toxicity study. Therefore, this project aims to determine the toxicology, molecular regulation of toxicity, pharmacokinetics and clastogenicity profiles of BZD9L1 in *in vitro* or *in vivo* models. This study comprises acute and subacute oral toxicity assessments, molecular toxicity evaluation, bone marrow chromosomal aberration and micronucleus assays, oral pharmacokinetics and *in vitro* mitochondrial toxicity assessments. BZD9L1 demonstrated no sign of toxicity at the limit dose (2000 mg/kg) in the acute toxicity study. Subacute toxicity data

highlighted the no-observed-adverse-effect level (NOAEL) for BZD9L1 up to the maximum dose of 1000 mg/kg. Although the alterations of some haematology and serum biochemistry parameters may not be biologically and clinically significant in this study. BZD9L1 regulated SIRT 1-7 protein expressions in the liver and kidney tissues and showed sex-specific inhibition of liver Cytochrome P450 (CYP) 2A5 and CYP2D proteins. However, BZD9L1 at all doses did not induce the molecular expression of organ injury markers or alter the cellular function markers in the liver and kidneys. BZD9L1 at doses up to 1000 and 2000 mg/kg also did not induce chromosomal aberration and bone marrow toxicity. In addition, no alteration of polychromatic erythrocytes (PCE)/total erythrocytes, or micronucleated PCE were observed, thereby delineating BZD9L1 to be non-clastogenic ($p > 0.05$). Plasma obtained from Sprague Dawley rats post-treated with a single oral dose of BZD9L1 at 250 mg/kg exhibited T_{max} (Time to Maximum concentration observed) at 4 h with C_{max} (Maximum Concentration observed) at 0.5 $\mu\text{g/mL}$. Overall, the present study highlights evidence on the safety of BZD9L1 in the short-term toxicity study and emphasizes the need for personalized strategies should BZD9L1 proceed down the drug discovery pipeline.

CHAPTER 1

INTRODUCTION AND LITERATURE REVIEW

1.1 Introduction

The rapid escalation of cancer incidence and the incremental mortality rate have made cancer a global burden. Cancer is the second most common cause of disease and is ranked as the leading cause of mortality worldwide (World Health Organization, 2020) with approximately 19.3 million new cancer cases and 10 million death cases were estimated in 2020 (GLOBOCAN, 2020, Sung et al., 2021). It is postulated to increase to 30.2 million new cases and 16.3 million death cases by 2040 (World Health Organization, 2021). The current regimes in cancer treatment including surgery, radiotherapy, chemotherapy, immunotherapy and endocrine therapy, have improved patient survival rates. However, the emergence of resistance to therapies, low overall survival rate, increased recurrence, and adverse side effects are still immense challenges in cancer treatment.

Constant expansion of knowledge and understanding toward the processes underlying cancer genesis enabled swift development in targeted therapy and revolutionised cancer treatment. Molecular targeted therapy has gained popularity in recent years, as precision drug delivery has been shown to have fewer side effects in patients than conventional chemotherapies (De Palma and Hanahan, 2012, Lee et al., 2018). Furthermore, many studies have demonstrated its positive outcomes in various malignancies, including breast cancer, gastric cancer, colon cancer, and acute myeloid leukaemia.

Benzimidazole is considered a crucial pharmacophore in cancer drug discovery due to their versatile mechanisms to hamper tumour progression (Shrivastava et al., 2017, Shimomura et al., 2019). Benzimidazole is a heterocyclic aromatic compound

formed by fusion of benzene with an imidazole ring. Its active indole core has a structure similar to the natural nucleotide, allowing it to interact noncovalently with a wide range of biological targets, thus, having an essential role in the drug and pharmaceutical industry (Purushottamachar et al., 2019). Due to their unique pharmacophore, straightforward synthesis strategies, and low toxicities, benzimidazole and its derivatives have also been widely applied in various pharmaceutical sectors as anti-hypertensive, anti-inflammatory, anti-bacterial, anti-fungal, anti-helminthic, anti-viral, anti-oxidant, anti-ulcer, and as a modulator of psychoactivity (Shaker et al., 2015, Tahlan et al., 2019).

Known as the molecular fountain of youth, sirtuins (SIRT) have garnered much attention in the past years. SIRT have been shown to reverse ageing and are lately linked to various metabolic diseases, including cancer, neurodegenerative diseases, diabetes, and cardiovascular diseases, making SIRT an attractive target for the development of pharmaceuticals (Bosch-Presegué and Vaquero, 2014). Furthermore, overexpression of SIRT proteins has been reported in various cancer types such as prostate, pancreatic, acute myeloid leukaemia, and colon cancers (Bosch-Presegué and Vaquero, 2011, Lee et al., 2021). SIRT can provide tumour cell survival advantage and resistance to therapy by inhibiting apoptosis, resisting senescence, prolonging lifespan and allowing unchecked cell division (Bosch-Presegué and Vaquero, 2011, Carafa et al., 2019). Although a number of SIRT inhibitors have been developed, these SIRT modulators vary in potency and target selectivity in different tissue types. Therefore, the search for more selective and potent SIRT modulators to treat cancer remains one of the most hyped areas of present-day research.

It has recently reported a benzimidazole derived small molecule SIRT inhibitor, BZD9L1, as a potential molecular targeted therapy agent. BZD9L1

demonstrated promising and specific anticancer effects by inhibiting SIRT1 and SIRT2 in colorectal (CRC) cancerous cells and tumour xenograft (Yoon et al., 2015, Tan et al., 2018, Tan et al., 2019, Tan et al., 2021). Despite the demonstration of potent anticancer effects *in vitro* and *in vivo*, one of the most significant challenges in drug development is the unpredictable nature of most forms of drug toxicity that might arise from the compound itself or the by-products of drug metabolism and detoxification processes. The toxicity that occurs can lead to the failure of new drug candidates in the preclinical toxicity assessment. Ensuring drug safety before testing in humans is central to drug development. Thus, *in vivo* toxicology is the proposed first step to investigate the toxic profile of BZD9L1 through different doses and time points to establish the subsequent adverse effects and levels of toxicity in the animal model.

This present study reports the preliminary evaluation of acute and subacute toxicities *in vivo* after oral exposure to BZD9L1. Furthermore, this study provides an insight into the molecular basis of BZD9L1 involved in the regulation of toxicity and metabolism after 28 days of repeated oral dose treatment *in vivo*. Furthermore, the clastogenicity and mitochondrial toxicity are the two important safety aspects enabling Go/No Go decisions in early drug discovery that have also been investigated in this study. Last, pharmacokinetic (PK) studies are integral to drug discovery to guide dosage selection, improve pharmacological effects, and minimise adverse events. These different studies are packaged to evaluate the safety and potential development of BZD9L1 as a therapeutic agent.

1.2 Literature review

The literature review mainly (i) describes the concept of molecular targeted therapy, (ii) provides a short overview of SIRTs and their role, (iii) provides recent

findings on benzimidazole and its derivatives as anti-cancer agent, (iv) outlines the importance of toxicology in drug development pipelines, and (v) reports the research achievement of BZD9L1 SIRT6 inhibitor.

1.2.1 Molecular targeted therapies

The brief introduction for molecular targeted therapies was extracted from the published review entitled “Molecular targeted therapy: treating cancer with specificity” (Lee et al., 2018). Molecular targeted therapy refers to the use of drugs or other substances as a therapeutic strategy that targets specific molecules (molecular targets) or biological pathway(s) to block the growth and spread of cancer cells, leading to the regression or destruction of cancer (Mocellin et al., 2005, Lee et al., 2018). The concept for targeted therapy was derived from the idea of “magic bullet” which Paul Ehrlich first coined in late 1800 (Ehrlich, 1906). It was initially used to depict the ability of a chemical that targets microorganisms specifically. Further development of the method was then expanded to cancer treatment (Brodsky, 1988).

The identification of ideal targets is imperative for the successful development of molecular targeted therapies in cancer. One consensus for cancer is due to the alteration of the genetic profile that leads to mutation or changes in proteins and receptors that favor cell survival and proliferation. These specific genetic alterations that distinguish cancer cells from normal cells can be used as molecular targets in developing molecularly targeted drugs (Røsland and Engelsen, 2015). By understanding the physiology and characteristic of specific molecular targets in cancer, researchers can identify potential molecular strategies to inhibit tumour growth and progression. Cancer markers can be identified using sequencing technology that enables researchers to compare the expression of genes and proteins between normal

and malignant cells to identify changes in gene and protein expressions (Vogelstein et al., 2013). Furthermore, a variety of cancer genomes can be sequenced through sequencing technology to reveal the genetic heterogeneity between malignant and normal cells within an individual, which is important to identify potential molecular targets for drug development (De Palma and Hanahan, 2012, Padma, 2015).

In general, the agents used in molecular targeted therapy can be divided into small molecules, monoclonal antibodies, immunotherapeutic cancer vaccines, and gene therapy (Padma, 2015, National Cancer Institute, 2017). Drugs used in molecular targeted therapy can function in several ways through the blockade of signals that promote cancer cell growth, interference with the regulation of cell cycle, and the induction of cell death to kill the cancer cells (Padma, 2015). In addition, drugs can be targeted at cancer cells or constituents within the tumour microenvironment to activate the immune system (Amer, 2014). Through their specific actions, the drug function by hampering tumour progression and invasion or resensitising resistant tumours to other treatment moieties when used as adjuncts (Tsai et al., 2014). The mode of action of molecular targeted therapy is illustrated in Figure 1.1.

The details on various type of molecular targeted therapy mechanism and agents were substantially discussed in the article (Lee et al., 2018). Despite the high selectivity of these targeted therapy agents, a range of previously unknown and sometimes unpredictable side effects can emerge, which has been extensively reviewed by Widakowich and colleagues (Widakowich et al., 2007).

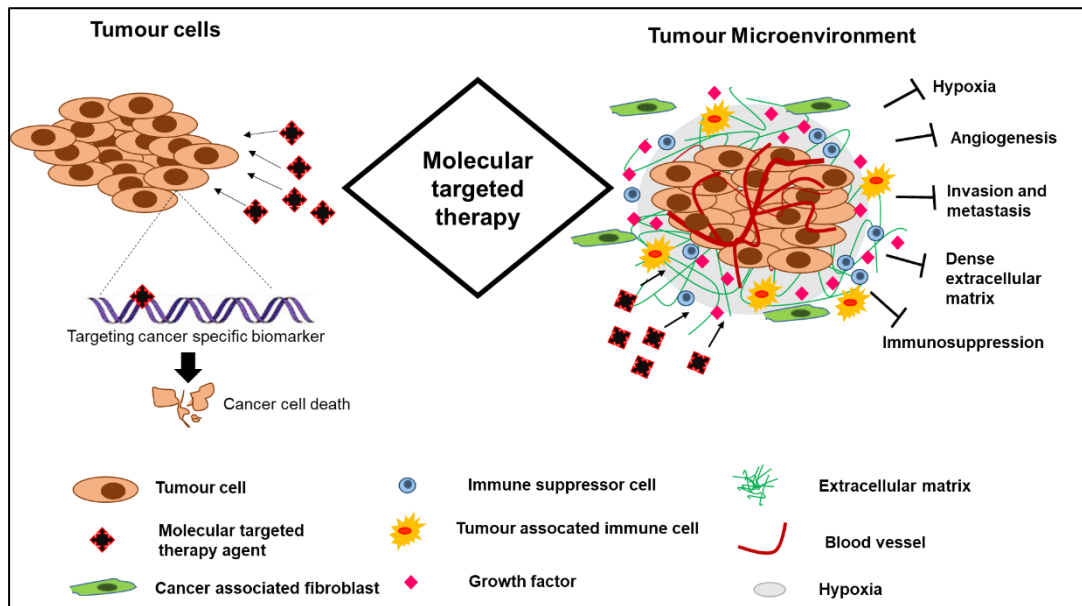


Figure 1.1 Overview of the molecular targeted therapy mechanism.

Molecular targeted therapy on cancer focuses on targeting specific cancer-associated molecules that are highly expressed in cancer cells or by modulating the tumour microenvironment related to tumour vasculature, metastasis or hypoxia. Image from Lee et al., 2018.

1.2.2 Sirtuins (SIRTs)

Sirtuins or silent mating type information regulation 2 homolog (SIRTs) are nicotinamide adenine dinucleotide (NAD)-dependent histone deacetylase (HDAC) and/or ADP ribosylase proteins that target both histone and non-histone proteins (Saunders and Verdin, 2007, Martínez-Redondo and Vaquero, 2013). SIRTs are highly conserved from bacteria to humans. They are homologs to the silencing information regulator 2 (Sir2) family, which initially originated from yeast, *Saccharomyces cerevisiae*, family, which plays critical roles in response to DNA damage and longevity in yeast (Bosch-Presegué and Vaquero, 2011, Kane and Sinclair, 2018). Mammalian SIRTs comprise of seven family members (SIRT1-7), varied in specificity, catalytic activity, localisation, and substrates. These SIRTs members share a catalytic domain of ~275 amino acids with variable lengths of unique additional N-terminal and/or C-terminal sequences (Michan and Sinclair, 2007, Saunders and Verdin, 2007, Yuan and

Marmorstein, 2012, Sanders et al., 2010). In general, the catalytic core domain of SIRT comprises a large and structurally homologous Rossmann-fold domain for NAD⁺/NADH binding proteins; a smaller zinc binding domain with four cysteine residues; and several loops (flexible loops or cofactor binding loop) connecting the two domains (Figure 1.2) (Sanders et al., 2010, Yuan and Marmorstein, 2012, Moniot et al., 2012).

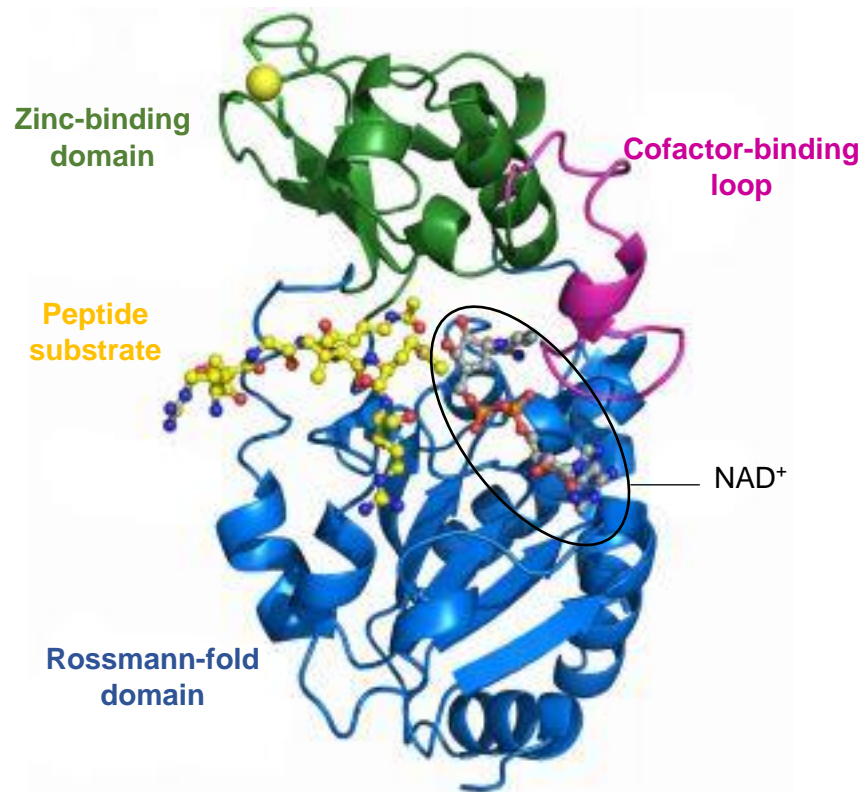


Figure 1.2 Representative SIRT structure.

Structure of human SIRT3 with the acetylCoA synthetase 2 (AceCS2) peptide and the NAD⁺ analog. The structure showed that the SIRT comprise of Rossmann-fold domain (blue), Zinc-binding domain (green), and cofactor binding loop (magenta) in a closed conformation. The active site of SIRT3 showed the binding of peptide substrate (yellow) and a carba-NAD molecule (grey). The image is adapted and modified from Moniot et al., 2012.

The SIRT proteins have distinct subcellular localisation where SIRT1 is prominently present in the nucleus but also found in the cytosol; SIRT2 in the cytoplasm (but may shuttle to the nucleus during cell division); SIRT3-5 mainly mitochondrial; SIRT6 in the nucleus and SIRT7 in the nucleolus (Michan and Sinclair, 2007, Alhazzazi et al., 2011).

Protein deacetylation plays a vital role in various regulatory processes. Histone deacetylation represses gene transcription, whereas non-histone proteins deacetylation can affect multiple physiologic activities and cellular functions, leading to a range of diseases, including cancer (Peng and Seto, 2011). SIRT is a class III protein deacetylase family that utilise NAD^+ as a cofactor to sense energy fluctuations resulting from oxidative, metabolic or genotoxic stress followed by the coordination of appropriate responses (Imai et al., 2000, Alhazzazi et al., 2011). In brief, the catalytic reaction of SIRT can be divided into two stages. First, SIRT binds to the acetyl group of protein residues, followed by the binding of NAD^+ , forming an enzyme- NAD^+ -N-acetylated substrate ternary complex, inducing the cleavage of nicotinamide (NAM) and production of the O-alkylamide intermediate. Subsequently, the nicotinamide ribose 2'-OH group binds to the O-alkylamide intermediate to yield one 2'-O-acetyl-adenosine diphosphate-ribose (2'-OAADPR) and one deacetylated lysine product (Shi et al., 2013, Kupis et al., 2016, Lin, 2018). Therefore, deacetylation of SIRT hydrolyses one NAD^+ to generate one NAM, one 2-O-acetyl-ADP-ribose, and one deacetylated protein substrate.

Among the seven members of the SIRT family, SIRT1-3 have exhibited robust deacetylation activity, while SIRT4-7 displayed weak or undetectable deacetylation activity (Saunders and Verdin, 2007, Lin, 2018, Du et al., 2011). In addition, SIRT4 and SIRT6 have been reported to possess ADP-ribosyl transferase activity, which was

believed to be the continued activity after deacetylation (Saunders and Verdin, 2007). Besides, SIRT6 has also been involved in other enzymatic activities including desuccinylation, demalonylation, deglutarylation, demyristoylation and lipoamidase processes (Kupis et al., 2016, Lin, 2018). The different catalytic properties of SIRT6 in turns categorised the SIRT6 to different classes according to their enzyme catalytic activities: Class I, strong deacetylation (SIRT1-3); Class II, ADP-ribosylation activity (SIRT4), Class III, demalonylation and desuccinylation activity (SIRT5) and Class IV, weak deacetylase and ADP-ribosylase activity (SIRT6-7) (Kincaid and Bossy-Wetzel, 2013). The enzymatic roles of SIRT6 for deacetylation, ADP-ribosylation and deacylation are illustrated in Figure 1.3-1.5.

SIRT6 are highly conserved enzymes implicated in transcriptional repression, which involved many biological processes linked to longevity, ageing, DNA repair, epigenetic regulation, metabolism homeostasis, and cell-environment communication (Bosch-Presegué and Vaquero, 2011, Bosch-Presegué and Vaquero, 2014). The latest study has shown that alternating splicing in the SIRT6 gene resulted in different isoforms that vary in expression level and localisation, giving differential effects on the biological functions mentioned above (Figure 1.6-1.7) (Zhang et al., 2021). Generally, SIRT6 functions can be classified into four main processes: chromatin regulation, cell survival under stress, metabolic homeostasis regulation, and developmental and cell differentiation (Bosch-Presegué and Vaquero, 2014).

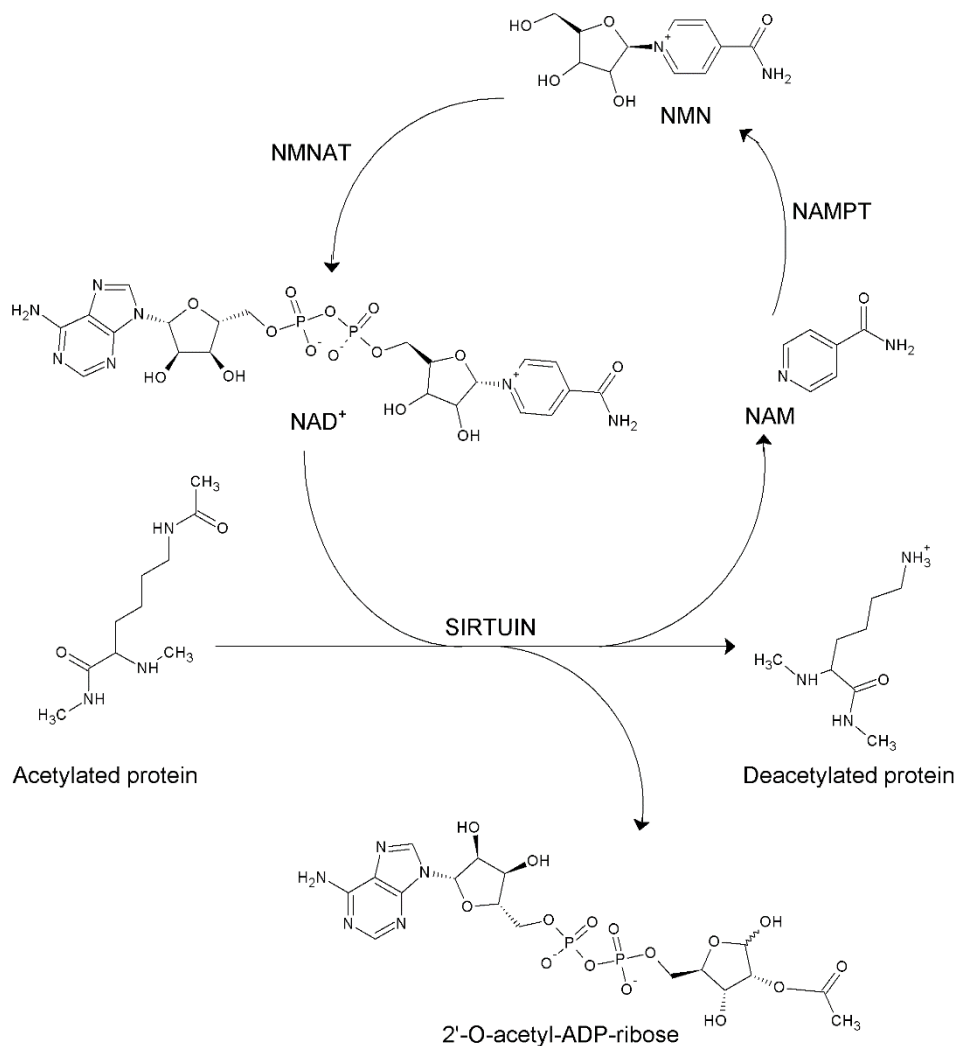


Figure 1.3 Enzymatic activities of SIRT deacetylation.

Mechanism of deacetylation. In stage 1, SIRT-mediated deacetylation by cleaving NAD⁺ yields an O-alkylamidate intermediate. In stage 2, the nicotinamide ribose 2'-OH group attacks the intermediate, produces 2'-O-acetylADP-ribose (2'-OAADPR) and deacetylated protein. Image is reproduced from Kupis et al., 2016 using ChemSketch. NAD⁺, nicotinamide adenine dinucleotide; NAM, nicotinamide; NAMPT, nicotinamide phosphoribosyltransferase; NMN, nicotinamide mononucleotide; NMNAT, nicotinamide mononucleotide adenylyltransferase

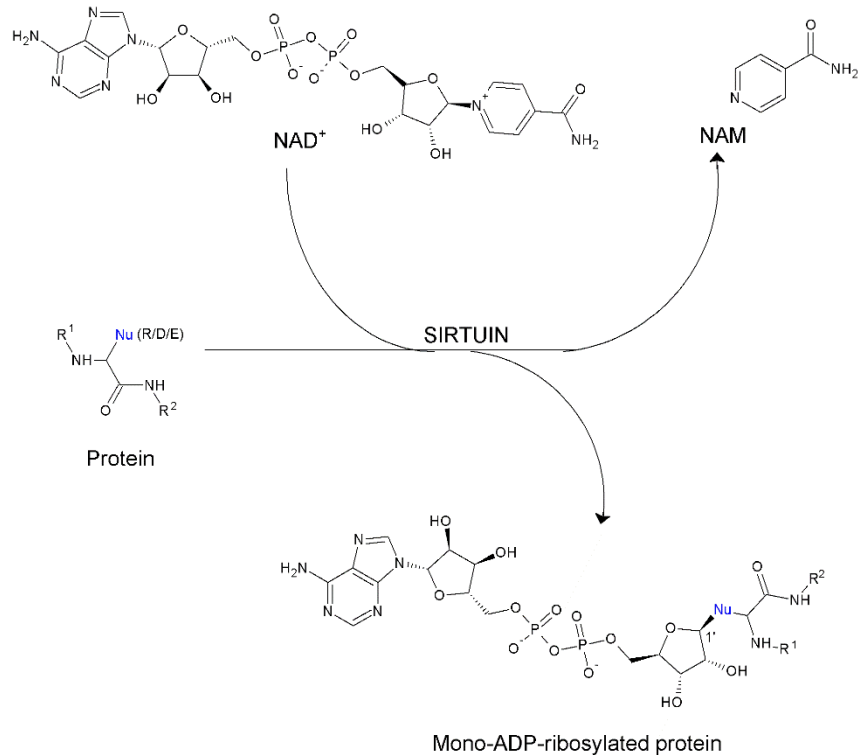


Figure 1.4 SIRT4 and SIRT6 exhibit ADP-ribosyl transferase activity.

SIRT4 and SIRT6 mediating the ADP-ribosylation involve the cleaving of NAD^+ , and transfer of an ADP-ribose group to proteins' side chains with nucleophilic group: Arg (R), Aspartic acid (D), and Glutamic acid (E). Image is reproduced from Kupis et al., 2016 using ChemSketch. NAD^+ , nicotinamide adenine dinucleotide; NAM, nicotinamide

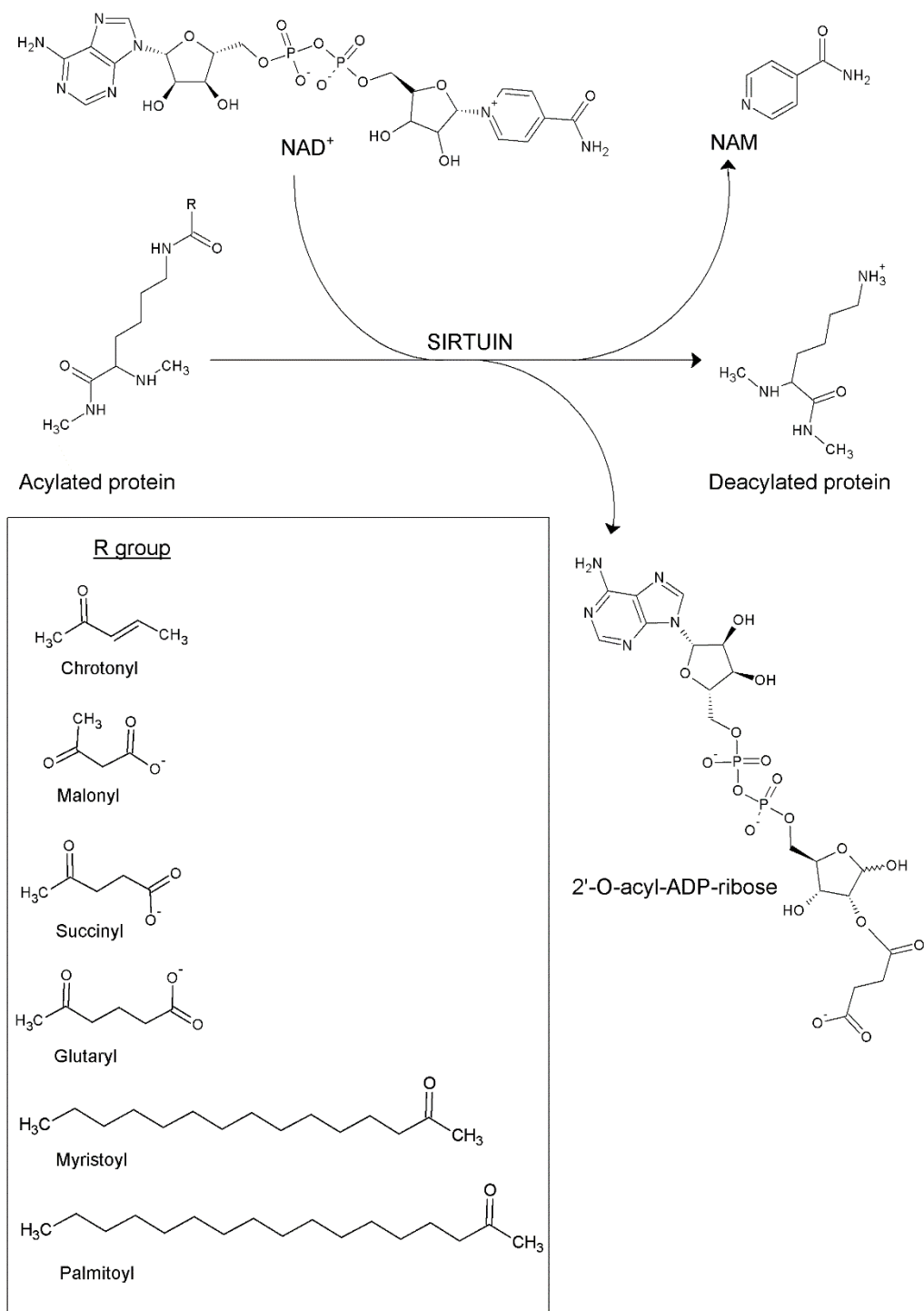


Figure 1.5 Enzymatic activities of SIRT deacylation.

SIRT-mediated deacylation by cleaving NAD⁺ to yield an O-alkylamidate intermediate. In stage 2, the nicotinamide ribose 2'-OH group attacks the intermediate, produces 2'-O-acyl-ADP-ribose and deacylated protein. Image is reproduced from Kupis et al., 2016 using ChemSketch. NAD⁺, nicotinamide adenine dinucleotide; NAM, nicotinamide

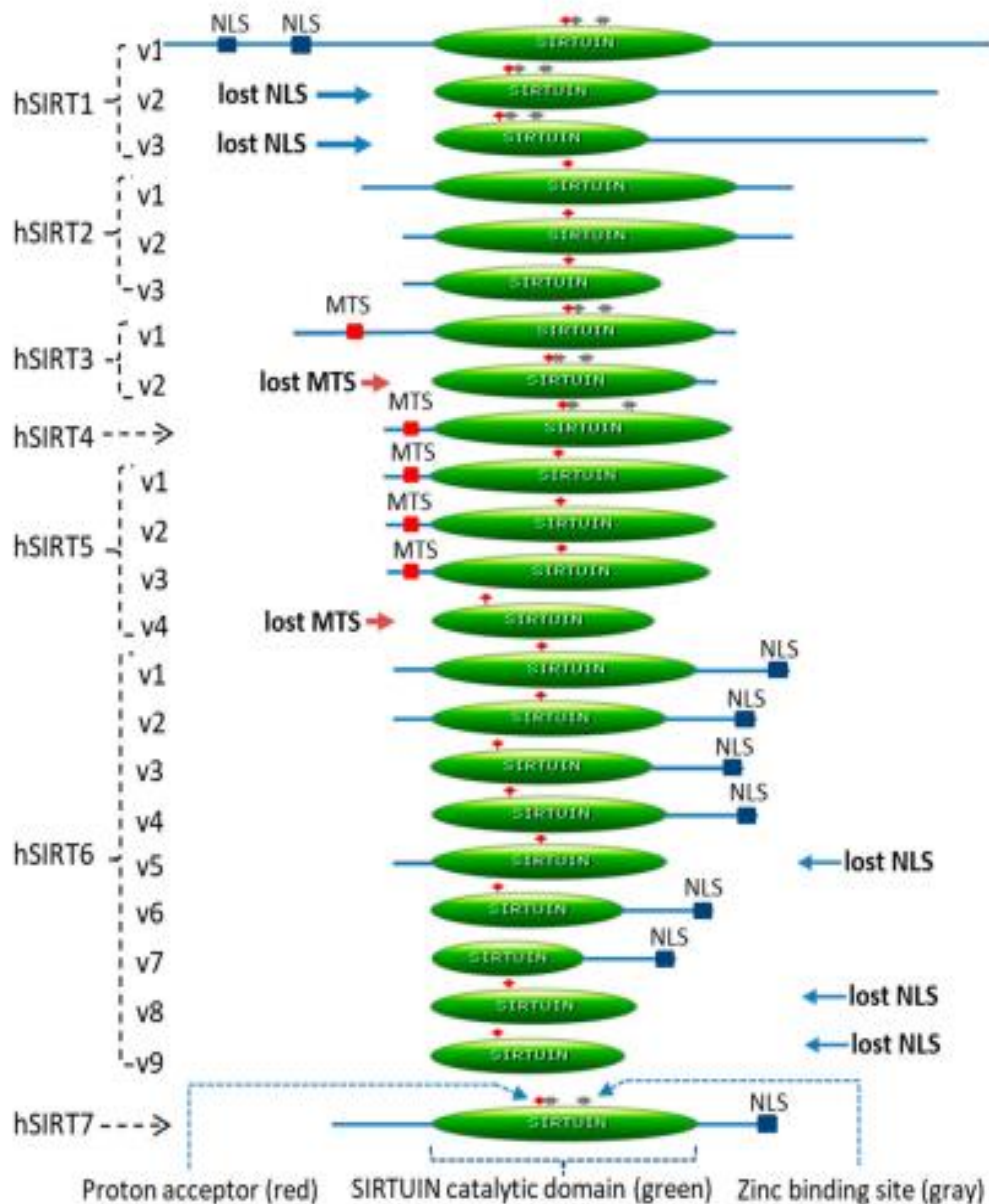


Figure 1.6 The 23 isoforms of SIRT1-7.

Human SIRT1-7 comprise seven members with isoforms that may exhibit loss of the N- or C-terminus, catalytic domain (green colour), nuclear localisation signal (NLS), or mitochondrial targeting signal (MTS). SIRT4 and SIRT7 have only one isoform. SIRT3 isoform v2 and SIRT5 isoform v4 possess the loss of MTS. The SIRT1 isoforms v2 and v3, the SIRT6 isoforms v5, v6, v8, and v9 have a loss of NLS. SIRT1 isoforms v2 and v3, the SIRT6 isoforms v5, v6, v8, and v9 have a loss of NLS. SIRT1 isoforms v2 and v3, the SIRT6 isoforms v5, v6, v8, and v9 have a loss of NLS. SIRTs with loss of MTS or NLS may be unable to enter the mitochondrial or nucleus. Image from Zhang et al., 2021.

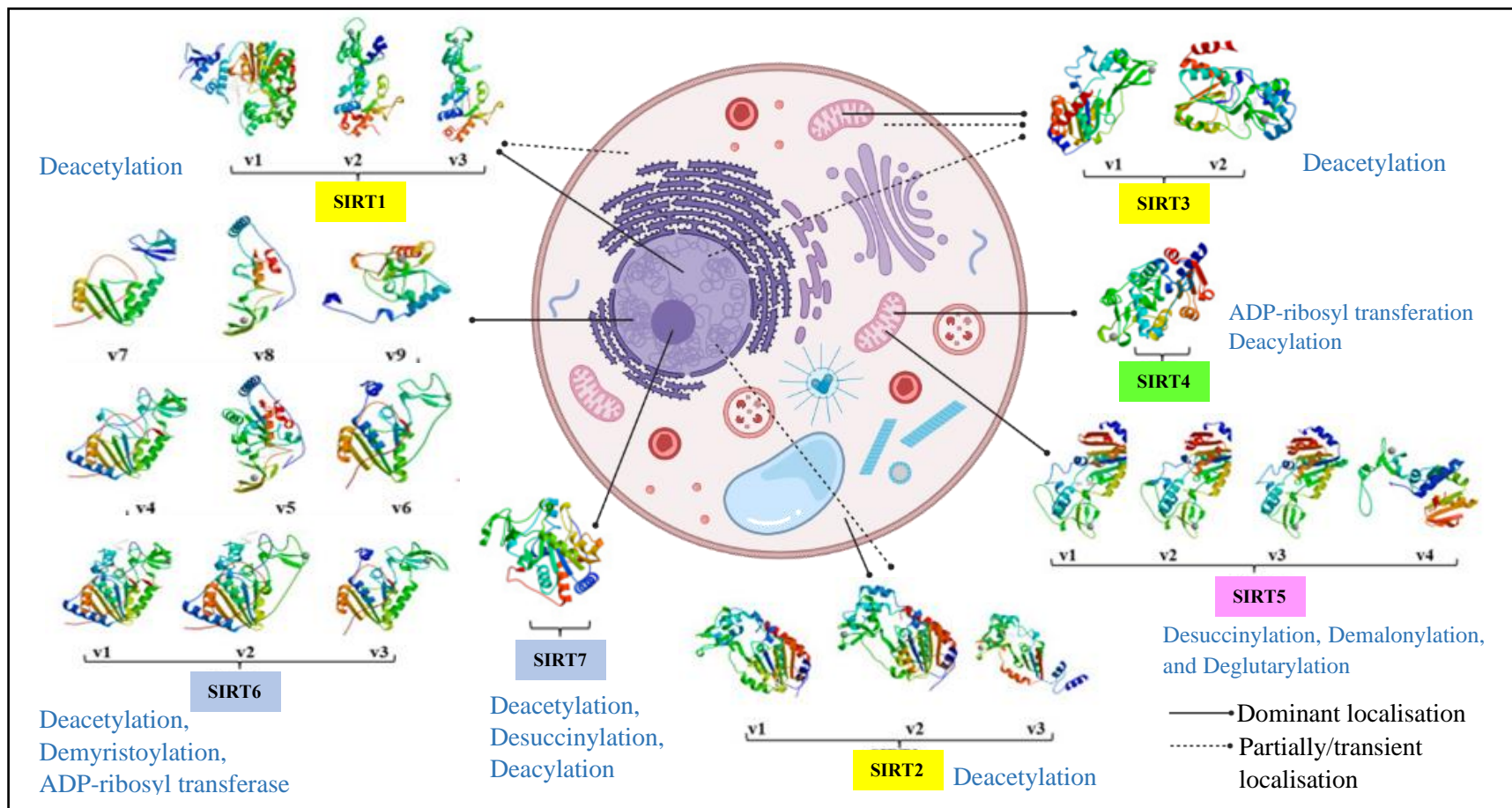


Figure 1.7 Overview of localisation, class and enzyme activities, and various isoforms of SIRT1-7.

The structure of SIRT protein with various alternative splicing was adapted and modified from Zhang et al., 2021. The image was created using PAINT and Biorender.com. Class 1: yellow box, Class 2: green box, Class 3: Purple box, and Class 4: navy blue box.

The following sections briefly introduce the seven members of the SIRT family and their role in cellular functions.

SIRT1

SIRT1 is by far the most extensively studied SIRT among the seven members of the SIRT family. SIRT1 is predominantly found in the nucleus, but the latest findings found the existence of two SIRT1 isoforms: SIRT1 isoform v2 and v3 reside in the cytoplasm (Zhang et al., 2021b). SIRT1 is highly detected in the testis, ovary, muscle, liver, pancreas, and adipose tissues and is predominantly located in the nucleus (Shoba et al., 2009). SIRT1 acts as a deacetylase targeting various substrates involved in modulation of cell metabolism, chromatin and epigenetic regulation, DNA repair, and stress responses (Nakagawa et al., 2009, Dang, 2014). SIRT1 plays a vital role in the regulation of chromatin structure by deacetylating the histones H4K16Ac, H3K9Ac, and H1K26Ac and promotes H3K9me3 methylation, thus, monitor facultative heterochromatin formation (Bosch-Presegué and Vaquero, 2011). SIRT1 has also been reported to deacetylate non-histone proteins such as pGC1 α , NF- κ B, FOXO1, FOXO3, FOXO4, Notch, HIF1 α , 14-3-3, PI3K, DNMT1, TORC1, HSF1, Ku70, STAT3. It is also involved in the silencing of gene transcription, mitochondria regulation, insulin signaling, gluconeogenesis, fatty acid oxidation, tumorigenesis, apoptosis, cell proliferation, survival, tissue regeneration, differentiation, inflammation and stress responses (Yu and Auwerx, 2010, Dang, 2014).

SIRT2

SIRT2 mainly resides in the cytoplasm but nucleo-cytoplasm translocalisation happens under certain circumstances. SIRT2 possess three main isoform SIRT2 isoform

1, isoform2 and isoform 3 (Maxwell et al., 2011, Zhang et al., 2021b). SIRT2 functions as a deacetylase involved in the regulation of chromatin assembly, the promotion of chromosomal stability, and the interaction with histone methyltransferase PR-Set7 (Inoue et al., 2007, Inoue et al., 2009, Vaquero et al., 2006, Serrano et al., 2013). SIRT2 also co-localised with microtubule functions in the deacetylation of α -tubulin at lysine 40 for cytoskeleton modulation (Machado de Oliveira et al., 2012). However, the mechanism of SIRT2 on microtubules deacetylation remains unclear. In addition, SIRT2 transiently migrates to the nucleus to regulate mitotic processes, control the cell cycle during early metaphase checkpoint regulation by deacetylating histone H4 at lysine 16 (Machado de Oliveira et al., 2012). Generally, SIRT2 deacetylates various substrates involved in the modulation of the cell cycle, including H4K16, p53, p65, FOXO1, FOXO3, and CDK4 (Zhao et al., 2019). SIRT2 also deacetylates FOXO1, and FOXO3 cell motility, adipocyte differentiation, oxidative metabolism, and cell death (Inoue et al., 2007).

SIRT3

SIRT3 is an NAD⁺-dependent deacetylase that is mainly localised in the mitochondria and is found to be highly expressed in metabolically active tissues such as the liver, heart and kidneys (Lombard et al., 2007, He et al., 2012). Interestingly, Schler and co-workers reported that SIRT3 resides in the nucleus, cytoplasm, and mitochondrial in its full-length state and under normal cell growth conditions (Scher et al., 2007, Marcus and Andrabi, 2018). The full-length SIRT3 protein is inactive with a molecular weight of approximately 44 kDa and possesses 25 amino acids at its N terminus, where proteolytic cleavage is required for the release of the active enzyme (28 kDa) (Schwer et al., 2002, Scher et al., 2007, Iwahara et al., 2012, Kincaid and Bossy-Wetzel, 2013, Jin et al., 2009).

The 28 kDa isoform that reside in mitochondrial contributes to the main deacetylation of mitochondrial proteins, maintaining the mitochondrial integrity from stress such as hypoxia and ROS (Lombard et al., 2007, Scher et al., 2007, Marcus and Andrabi, 2018). SIRT3 also targets proteins in the nucleus, cytoplasm, and mitochondria (e.g., H4K16Ac, H3K9Ac, superoxide dismutase 2 (SOD2), FoxO3a,), to regulate intracellular processes including metabolism, longevity, aging, ROS homeostasis, energy production, thermogenesis, caloric restriction, cancer, apoptosis, and stress responses (Chen et al., 2014, Ansari et al., 2017).

SIRT4

SIRT4 is located mainly in the mitochondrial matrix with known ADP-ribosyltransferase activity, but lacks NAD⁺-dependent deacetylase activity (Haigis et al., 2006, Mahlknecht and Voelter-Mahlknecht, 2009). However, in a recent study, SIRT4 was reported to exhibit lysine deacetylase activity and displaying deacylation activity by removing acyl group such as acetyl, lipoyl, glutaryl, methylglutaryl, and hydroxymethylglutaryl adducts from lysine residues (Wood et al., 2018). Activation of SIRT4 required proteolytic cleavage at its NH₂- terminus to yield a 29 kDa SIRT4 protein (Ahuja et al., 2007). SIRT4 is widely distributed in all tissues, but is highly detected in the liver, testes, muscle, heart, brain, pancreas, and kidney cells which is consistent with their role in regulating cellular metabolic homeostasis involved in insulin secretion and fatty acid oxidation (Frye, 1999, Laurent et al., 2013b, Anderson et al., 2017, Min et al., 2019). In addition, SIRT4 plays an important role in regulating mitochondrial metabolism and DNA damage responses.

SIRT5

SIRT5 is one of the mitochondrial SIRT6s with isoform v1 and isoform v2 being the two main isoforms, whereas isoform v3 and isoform v4 have unknown physiological information (Matsushita et al., 2011, Kumar and Lombard, 2018, Du et al., 2018). SIRT5 demonstrated robust demalonylase and desuccinylase activities in comparison to deacetylase activity (He et al., 2012, Du et al., 2011). In the mitochondrial, SIRT5 is important in maintaining metabolic homeostasis by modulating the metabolic enzymes involved in the glycolysis, tricarboxylic acid cycle, FAO, and adenosine triphosphate (ATP) synthesis through (Nishida et al., 2015, Kumar and Lombard, 2018, He et al., 2021). Besides, SIRT5 activates the carbamoyl phosphate synthetase 1 (CPS-1) enzyme of the urea cycle to catalyse the conversion of ammonia to urea (Nakagawa et al., 2009), and plays a role in ketone body production (Rardin et al., 2013). Furthermore, SIRT5 also functions as a ROS scavenger to reduce oxidative stress and damages in the host cells and tissues (Lin et al., 2013).

SIRT6

SIRT6 is located primarily in the nucleus and bound to the chromatin. SIRT6 mainly functions in the regulation of metabolic homeostasis, maintain genome stability, and DNA repairs (Mostoslavsky et al., 2006, Lerrer et al., 2016). The latest study reported the presence of nine isoforms for SIRT6, but required a deeper study to investigate the physiological roles of these isoforms (Zhang et al., 2021b). SIRT6 exhibit nucleosome dependent- deacetylase activity on histone proteins (Gil et al., 2013). SIRT6 is a sensitive DNA damage sensor and play a significant role in DNA repair (McCord et al., 2009, Toiber et al., 2013, Bütepage et al., 2015). SIRT6 recruits the chromatin remodeler

SNF2H to DSB, deacetylates histone H3K56 at the break site, and regulates downstream DNA damage response (DDR) signalling (Toiber et al., 2013). In addition, SIRT6 activates the ADP-ribosyltransferase diphtheria toxin-like (ARTD1) enzyme through MARylation for base excision repair (Bütepage et al., 2015).

SIRT7

SIRT7 is the last deacetylase with the least studied found among the family and is localised in the nucleolus (Michishita et al., 2005). SIRT7 exhibits weak deacetylase activity as compared to the same nuclear-localised SIRT1 and SIRT6. SIRT7 deacetylates various substrates including p53, H3K18, H3K122, PAF53, U3-55K, NPM1, PGK1, CDK9, GABP β 1, FOXO3, DDX21 SMAD, involved in various biological functions including apoptosis, chromatin architecture homeostasis, ageing, metabolism, gene silencing, and genome stability (Wu et al., 2018). Controversial findings of SIRT7 on p53 deacetylation have also been reported in different cell types (Michishita et al., 2005, Vakhrusheva et al., 2008, Barber et al., 2012, Kim et al., 2013, Lv et al., 2017, Sun et al., 2018, Vakhrusheva et al., 2008). Besides the difference in mutation profile and tissue of origin of these cell type, the effect of SIRT7 on p53 activity may also act through the interaction with other molecules instead of direct deacetylation (Lu et al., 2020b, Yu et al., 2020, Ianni et al., 2021). SIRT7 is associated with the transcriptional machinery of RNA polymerase I (Pol I), regulating rRNA expression and the stress response (Chen et al., 2013). SIRT7 also possess desuccinylation activity on histone proteins, H3K122, promoting DNA double-strand breaks repair and cell survival (Li et al., 2016), Moreover, SIRT7 mediated deacylation of SP7/Osterix during bone formation.

Dysregulation of either one of the SIRT members could impair cellular function and result in tumorigenesis and many other diseases (Imai et al., 2000, Nakagawa and Guarente, 2011, Choi and Mostoslavsky, 2014, Carafa et al., 2019). Increasing pieces of evidence have demonstrated the crucial role of SIRT in cancer initiation and progression. Thus, SIRT has become the focus of increasing attention as potential targets in anticancer therapy (Carafa et al., 2019, Bosch-Presegue and Vaquero, 2014, Carafa et al., 2012, Bosch-Presegúe and Vaquero, 2011, Saunders and Verdin, 2007). The function of SIRT may be different depending on the cell-type and tumour-type; thereby, SIRT may act as a tumour promoter or suppressor. In the events of cellular stress, the opposite roles of SIRT can be exhibited for instance via the maintenance of DNA integrity (anti-tumour) versus promotion of cell survival under stress (pro-tumour) (Bosch-Presegúe and Vaquero, 2011, Lee et al., 2021). However, the specific factors in the cancer type and stroma underpinning the oncogenic or suppressor roles of SIRT are still unknown. The details of the dual roles of SIRT in cancer and the available SIRT modulators have been extensively reviewed in the published book chapter entitled “The bifunctional roles of sirtuins and their therapeutic potential in cancer.” (Lee et al., 2021).

1.2.3 SIRT expression in mouse

In the latest study, Zhang et al., reported that murine consists of 15 SIRT isoforms (Zhang et al., 2021b). The mouse has two SIRT1 isoforms that exhibit 100% homology to the human isoform 1 (Zhang et al., 2021b). However, no further information on the mouse isoforms is provided. Mouse SIRT2 comprises four isoforms: isoforms 1-3 (Maxwell et al., 2011) and a catalytic inactive isoform 5 (Rack et al., 2014). Furthermore, there are three SIRT3 isoforms in mice where isoform 1 and isoform 2 are predominant

in mitochondrial, while the SIRT3 isoform 3 protein appeared partially to be in mitochondria localisation (Yang et al., 2010). In contrast to humans, rodent has only one SIRT5 isoform (Du et al., 2018). Similar to humans, the rodents have only one isoform for SIRT4 and SIRT7. The literature search did not reveal information on the number of mice SIRT6 isoforms.

1.2.4 Limitations of commercially available SIRT inhibitors

This section was adapted and modified from the published book chapter entitle “The bifunctional roles of sirtuins and their therapeutic potential in cancer.” (Lee et al., 2021). Numerous SIRT inhibitors have been developed and available in the market such as EX527 (Selisistat), Sirtinol, AGK2, Tenovin-6, SirReal2, Cambinol, Salermide and Suramin. These SIRT inhibitors target either the NAD⁺ binding site or the acetylated peptide substrate-binding site on the active site of the SIRT protein (Schuetz et al., 2007, Gertz et al., 2013). However, most of the SIRT modulators have been reported to lack selectivity, requisite pharmacological properties and do not display a significant potency with high micromolar IC₅₀ concentration, ultimately limiting their potential for development as therapeutic agents. Growing evidence has indicated that the anticancer effects of available SIRT inhibitors such as Tenovin-6 can most likely be attributed to the non-specific targeting of multiple SIRTs at once (Lain et al., 2008, MacCallum et al., 2013, Ladds et al., 2020). This action may improve treatment outcomes but would also induce antagonist effects and unwanted toxicity consequences. Thus, the polypharmacology properties of SIRT inhibitors is an important factor to establish the feasibility of them in anticancer therapies. Additionally, among the SIRT inhibitors, only Tenovin (Lain et al., 2008), Cambinol (Heltweg et al., 2006), and Inauhzin (Zhang et al.,

2015) have demonstrated anticancer effects with no reported toxicity in *in vivo* models. At the same time, only limited number SIRT inhibitors have entered into clinical trials as possible anticancer agents. Suramin has been reported to be used as a combination treatment with doxorubicin in a phase I clinical trial to treat advanced solid tumours, including adrenocortical carcinoma, unspecified adult solid tumour, breast, colorectal and prostate cancers, and phase II for lung cancer (<https://clinicaltrials.gov>). However, the current status for Suramin remains unknown. EX527 is another SIRT1 inhibitor that reached phase II clinical trials but for the treatment of Huntington's Disease (Westerberg et al., 2015, Süßmuth et al., 2015). Therefore, research focused on developing a highly potent, specific, and low-toxicity SIRT inhibitors is crucial.

1.2.5 Benzimidazole as anticancer agents

Benzimidazole (also known as 1H-Benzimidazole, 1,3-benzodiazole, benzoglyoxaline, iminazole, and imidazole) is an aromatic organic compound that contains a benzene ring fused to an imidazole ring at the 4,5-position to form a bicyclic ring (Wright, 1951, Keri et al., 2015). Historically, benzimidazole was first synthesised by Hoebrecker, followed by Ladenberg and Wundt during 1872–1878 (Wright, 1951). Benzimidazole has a molecular weight of 118.14 g/mol and appears as white tabular crystals. Benzimidazole contains a hydrogen atom attached to nitrogen in the 1-position (Figure 1.8) and can form a tautomer upon interaction with aprotic solvents, such as water or the existence of more than one benzimidazole molecule (Wright, 1951). However, substitution at position N will prohibit the tautomerism process (Keri et al., 2015).

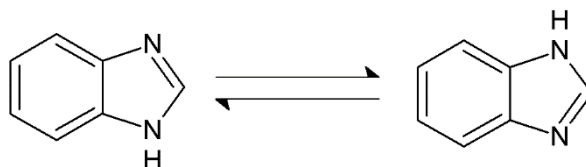


Figure 1.8 Structure and tautomerism of benzimidazole.

The structure was created using ChemSketch.

Benzimidazole is a weak base with pK_a values of 5.3 and 12.3 for pK_{a1} and pK_{a2} , respectively (Singh and Silakari, 2018). Benzimidazole ring is highly stable and can withstand extreme conditions such as being heated under pressure up to 270 °C in a concentrated sulphuric acid solution or vigorous treatment with hot hydrochloric acid or alkalis (Singh and Silakari, 2018).

Benzimidazole is an important biologically active heterocyclic compound that forms the pharmacophores of many drugs. Benzimidazoles have a structure that resembles naturally occurring purine nucleotide, which allows them to easily contact the biopolymers within the living system (Kamanna, 2019). With this unique structure advantage, benzimidazole and its derivatives are widely applied in the development of anticancer drugs. They may function as topoisomerase inhibitor, DNA intercalation and alkylating agents, androgen receptor antagonist, or inhibitors of Poly (ADP-ribose) polymerase (PARP), protein tyrosine kinase, dihydrofolate reductase, and microtubule (Shrivastava et al., 2017, Shimomura et al., 2019). Recently, benzimidazole derivatives have been reported to act as potent inhibitors of SIRT and murine double minute 2/X, demonstrating promising anticancer activities (Yoon et al., 2015, Tan et al., 2018, Tan et al., 2019, Mrkvová et al., 2019).

Literature search reveals a wealth of knowledge on the imperative roles of benzimidazole and its derivatives in targeting cancers. Benzimidazole is also in the top

ten most frequent five-members nitrogen heterocycles in U.S. FDA approved drugs (Vitaku et al., 2014). However, current benzimidazole drugs may lack specificity, i.e., targeting multi biomarkers which may result in the synergistic impediment of tumour growth and possibly induce antagonist effect on tumours. More downstream studies are needed to further investigate the molecular mechanism pathway and the consequence effects *in vitro* and *in vivo*. Due to its high similarity to naturally occurring nucleotides, benzimidazole and its derivatives can hijack multiple cellular processes at any one time. In addition, problems like toxicity, drug-resistant and poor bioavailability have become the limiting factors in the development of most benzimidazole derivatives for cancer treatment. This could explain the limited number of benzimidazole drugs having successfully entered clinical trials, let alone obtain FDA approval as potential anticancer agents.

1.2.6 Toxicology

Toxicology, traditionally, it is known as “the science of poison”, which is then referred to the scientific study and characterisation of the adverse effects of xenobiotics, which include biological, chemical or physical agents in a living organism (Langman and Kapur, 2006, Radenkova–Saeva, 2008, Ernst, 2015, Milles, 1999). The term, xenobiotic, originates from the Greek word *xenos* (foreign), and *bios* (life), meaning the foreign substances that enter the body (Ernst, 2015).

Philippus Aureolus Theophrastus Bombastus von Hohenheim – Paracelsus (1493-1541), is one of the well-known founders of modern toxicology and contributes to the history of science and medicine. Paracelsus has expressed the basics of toxicity with his famous quotes: “All things are poison and nothing are without poison; only the dose